Electronic Supplementary Information

Synthesis, derivatization and structural analysis of phosphorylated mono-, di- and tri-fluorinated D-gluco-heptuloses by glucokinase: tunable phosphoglucomutase inhibition

Jian-She Zhu,[†] Kyle M. Stiers,[‡] Sherany M. Winter,[†,|,#] Anthony D. Garcia,[†,▽,#] Antoine F. Versini,[†,⊥,#] Lesa J. Beamer,[†,*] and David L. Jakeman[*,†,§]

[†] College of Pharmacy, 5968 College Street, Dalhousie University, Halifax, Nova Scotia, B3H 3J5, Canada

[‡] Biochemistry Department, 117 Schweitzer Hall, University of Missouri, Columbia, Missouri 65211, United States

[|] Hogeschool Leiden (UAS Leiden), Department of Chemistry, Zernikedreef 11, 2333 CK Leiden, The Netherlands

[▽] École Nationale Supérieure de Chimie de Rennes, 11 Allée de Beaulieu, CS 50837, 35708 Rennes Cedex 7, France

[⊥] École Supérieure de Physique et de Chimie Industrielles de la Ville de Paris, 10 rue Vauquelin 75005, France

[§] Department of Chemistry, Dalhousie University, Halifax, Nova Scotia, B3H 4R2, Canada

***E-mail: David.Jakeman@dal.ca, and beamerl@missouri.edu**

Electronic Supplementary Information 1

Figure S1: ^{19}F {^{1}H} NMR (A) and ^{31}P {^{1}H} NMR (B) spectra comparison of phophonate 6 and phosphate 7. 3

Figure S2: Michaelis-Menten plots. (a) αPMM/PGM (b) G6PDH 4

Figure S3: IC_{50} data for the αPMM/PGM catalyzed formation of G6P from αG1P in response to inhibitors (1-4).... 5

Figure S4: IC_{50} data for the βPGM catalyzed formation of G6P from βG1P in response to inhibitors (1-4). 6

Figure S5. Sequence alignment of *Xanthomonas citri* PGM (top) and *P. aeruginosa* PMM/PGM (bottom). 6

Table S1. X-ray data collection and refinement statistics for the CH3G6P complex. (Statistics for the highest-resolution shell are shown in parentheses.) 7

Table S2. A comparison of protein-ligand hydrogen bonds of complex between the 1-XcPGM and αG1P. 9

Figure S6. ^{1}H NMR (300 MHz, $CDCl_3$) spectra of compound 9 10

Figure S7. ^{1}H NMR (500 MHz, D_2O) spectra of compound 12 11

Figure S8. ^{13}C NMR (125 MHz, D_2O) spectra of compound 12 11

Figure S9. ^{1}H NMR (500 MHz, D_2O) spectra of compound 1 12

Figure S10. ^{31}P NMR (202 MHz, D_2O) spectra of compound 1 12

Figure S11. ^{13}C NMR (125 MHz, D_2O) spectra of compound 1 13

Figure S12. ^{19}F NMR (470 MHz, DMSO-d^{6}) spectra of compound 10 13

Figure S13. ^{19}F NMR (470 MHz, D_2O) spectra of compound 13 14

Figure S14. ^{1}H NMR (500 MHz, D_2O) spectra of compound 2 14

Figure S15. ^{19}F NMR (470 MHz, D_2O) spectra of compound 2 15

Figure S16. ^{31}P NMR (202 MHz, D_2O) spectra of compound 2 15

Figure S17. ^{13}C NMR (125 MHz, D_2O) spectra of compound 2 16

Figure S18. ^{1}H NMR (500 MHz, $CDCl_3$) spectra of compound 6 16

Figure S19. ^{19}F NMR (470 MHz, $CDCl_3$) spectra of compound 6 17

Figure S20. ^{31}P NMR (202 MHz, $CDCl_3$) spectra of compound 6 17

Figure S21. ^{1}H NMR (500 MHz, $CDCl_3$) spectra of compound 7 18

Figure S22. ^{19}F NMR (470 MHz, $CDCl_3$) spectra of compound 7 18

Figure S23. ^{31}P NMR (202 MHz, $CDCl_3$) spectra of compound 7 19

Figure S24. ^{13}C NMR (125 MHz, $CDCl_3$) spectra of compound 7 19

Figure S25. ^{1}H NMR (500 MHz, $CDCl_3$) spectra of compound 8 20

Figure S26. ^{19}F NMR (470 MHz, $CDCl_3$) spectra of compound 8 20

Figure S27. ^{1}H NMR (500 MHz, D_2O) spectra of compound 14 21

Figure S28. ^{19}F NMR (470 MHz, D_2O) spectra of compound 14 21

Figure S29. ^{13}C NMR (125 MHz, D_2O) spectra of compound 14 22

Figure S30. ^{1}H NMR (500 MHz, D_2O) spectra of compound 3 22

Figure S31. ^{19}F NMR (470 MHz, D_2O) spectra of compound 3 23

Figure S32. ^{31}P NMR (202 MHz, D_2O) spectra of compound 3 23

Figure S33. ^{13}C NMR (125 MHz, D_2O) spectra of compound 3 24

Figure S34. ^{19}F NMR (470 MHz, $CDCl_3$) spectra of compound 11 24

Figure S35. ^{1}H NMR (500 MHz, D_2O) spectra of compound 15 25

Figure S36. ^{19}F NMR (470 MHz, D_2O) spectra of compound 15 25

Figure S37. ^{13}C NMR (125 MHz, D_2O) spectra of compound 15 26

Figure S38. ^{1}H NMR (500 MHz, D_2O) spectra of compound 4 26

Figure S39. ^{19}F NMR (470 MHz, D_2O) spectra of compound 4 27

Figure S40. ^{31}P NMR (202 MHz, D_2O) spectra of compound 4 27

Figure S41. ^{13}C NMR (125 MHz, D_2O) spectra of compound 4 28

References 28

Figure S1: ^{19}F {^{1}H} NMR (A) and ^{31}P {^{1}H} NMR (B) spectra comparison of phophonate 6 and phosphate 7.

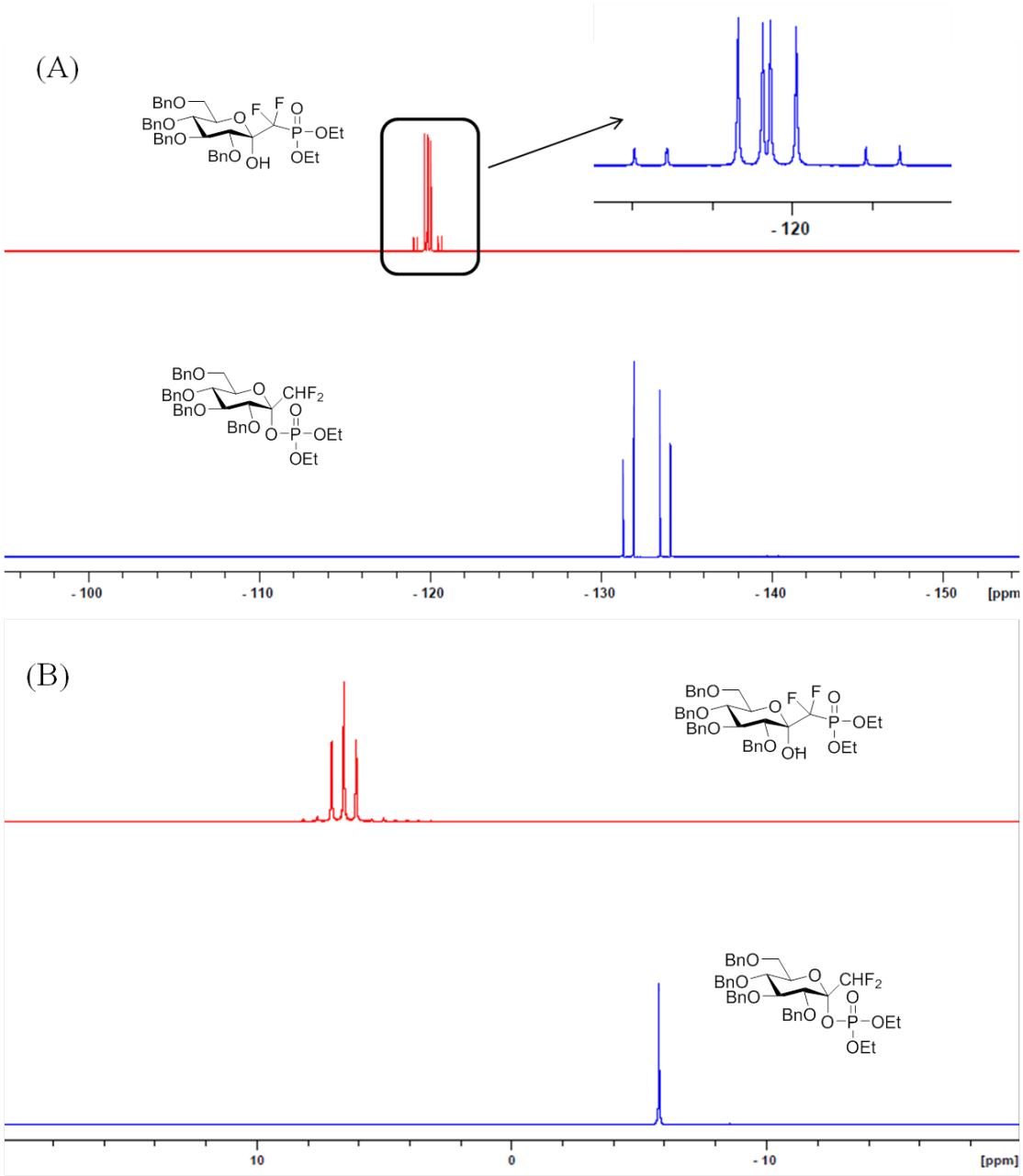

General kinetic inhibition assays of analogues 1-4 against αPMM/PGM and βPGM

Enzyme kinetic rates for αPMM/PGM and βPGM were determined using a coupled assay with glucose 6-phosphate dehydrogenase (G6PDH) to monitor G6P formation from G1P from G1P, using αG16BP[1] or α-fructose-1,6-bisphosphate (αF16BP)[2] as an activator of αPMM/PGM and βPGM, respectively (**Scheme S1**). G6PDH oxidized G6P to 6-phosphogluconolactone with reduction of NAD^+ to NADH, was monitored at 340 nm. Kinetic rates were recorded using a SpectraMax Plus UV/Vis spectrophotometer. Kinetic rates were monitored at A_{340} over 10 min at 25°C. The linear

portions of time progress curves were plotted using GraFit 5.0.4. Reactions were carried out in 96-well plates.

Scheme S1. Mechanistic schemes of PGM-G6PDH coupled assay

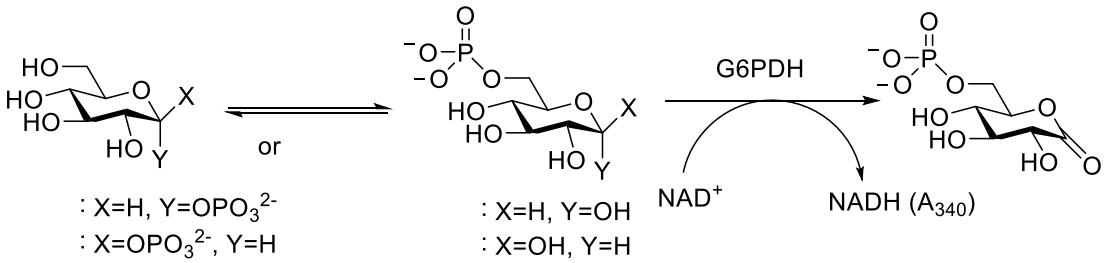

Enzyme kinetic determination for αPMM/PGM and G6PDH

Michaelis Menten kinetic data for αPMM/PGM was obtained using the conditions described for the αPMM/PGM IC_{50} experiment (without inhibitor present) with variable αG1P (0–200 μM). For the kinetic assay with G6PDH alone, it was carried out in a final volume of 200 μL containing 50 mM Hepes buffer pH 7.4, 0.5 mM NAD^+, 0.125 U/mL G6PDH, G6P (75–1000 μM).

Figure S2: Michaelis-Menten plots. (a) αPMM/PGM (b) G6PDH

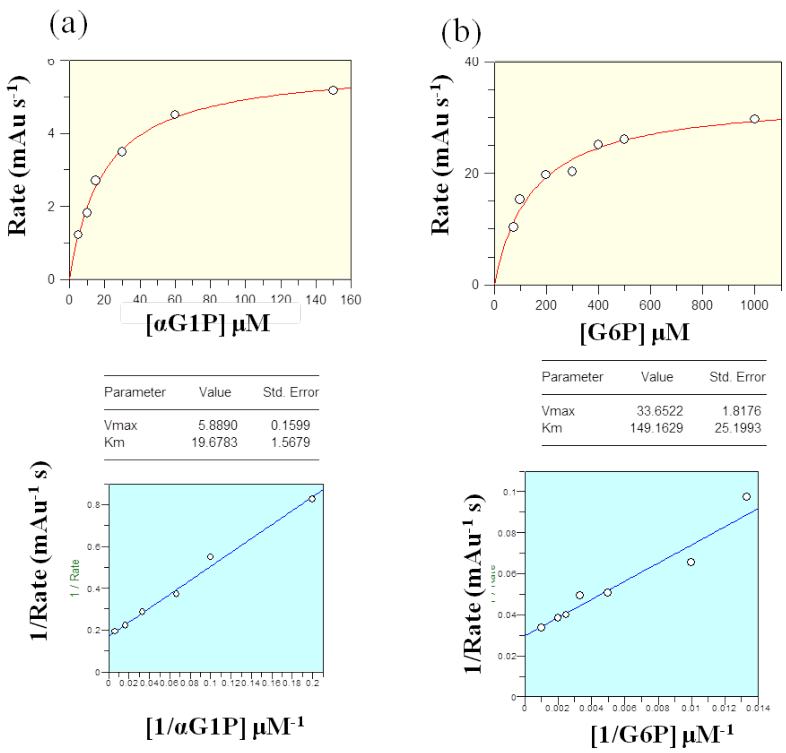

Figure S3: IC_{50} data for the αPMM/PGM catalyzed formation of G6P from αG1P in response to inhibitors (1-4).

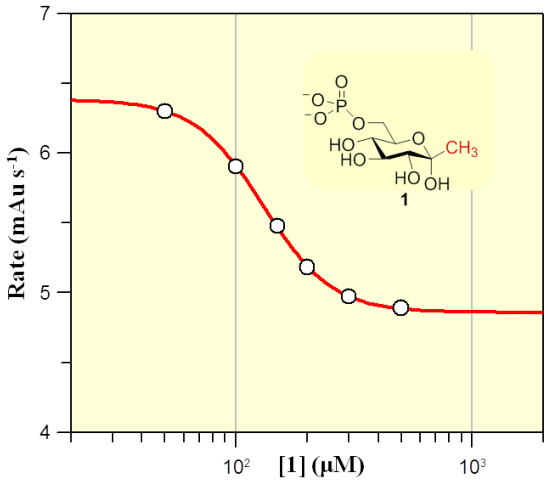

Parameter	Value	Std. Error
Y Range	1.5231	0.0156
IC 50	130.5779	1.2334
Slope factor	2.9929	0.0820
Background	4.8579	0.0110

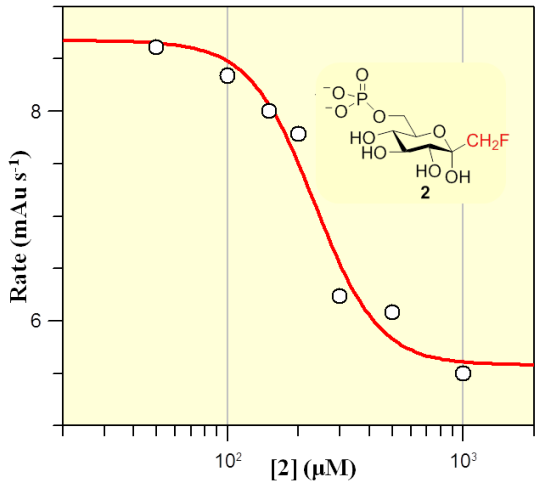

Parameter	Value	Std. Error
Y Range	3.0952	0.3676
IC 50	233.6152	27.8481
Slope factor	3.1798	0.9536
Background	5.5773	0.2796

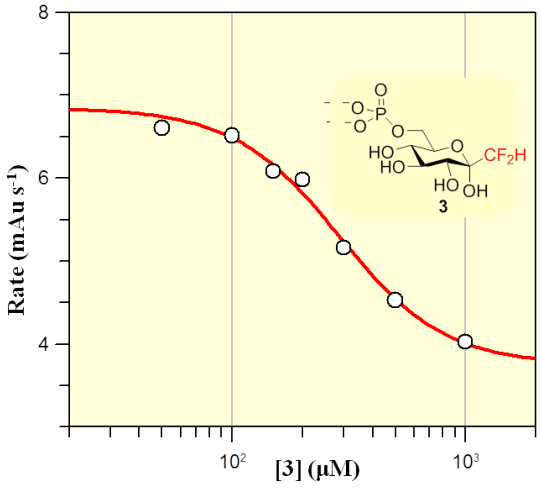

Parameter	Value	Std. Error
Y Range	3.0941	0.3249
IC 50	288.0001	36.8119
Slope factor	1.9220	0.3621
Background	3.7498	0.2720

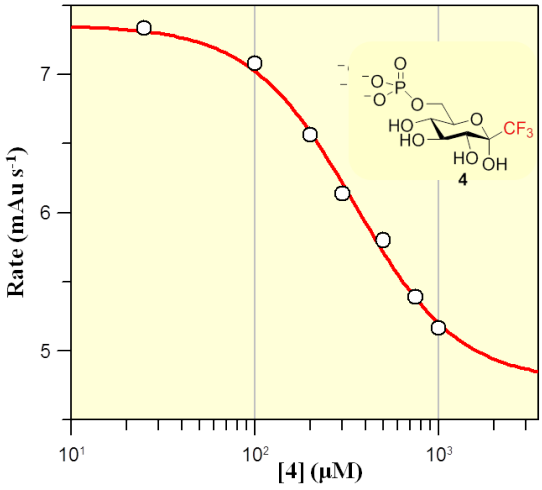

Parameter	Value	Std. Error
Y Range	2.5729	0.2836
IC 50	346.9459	54.7253
Slope factor	1.5425	0.2591
Background	4.7802	0.2584

Figure S4: IC_{50} data for the βPGM catalyzed formation of G6P from βG1P in response to inhibitors (1-4).

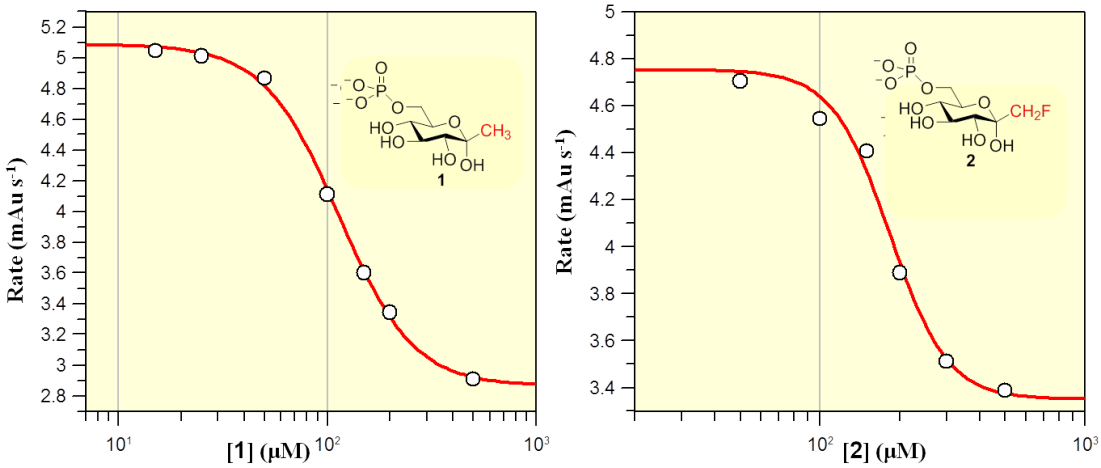

Parameter	Value	Std. Error
Y Range	2.2232	0.0592
IC 50	113.2041	3.4058
Slope factor	2.4330	0.1680
Background	2.8636	0.0484

Parameter	Value	Std. Error
Y Range	1.4019	0.1439
IC 50	183.4089	14.2259
Slope factor	4.0115	1.1117
Background	3.3504	0.1134

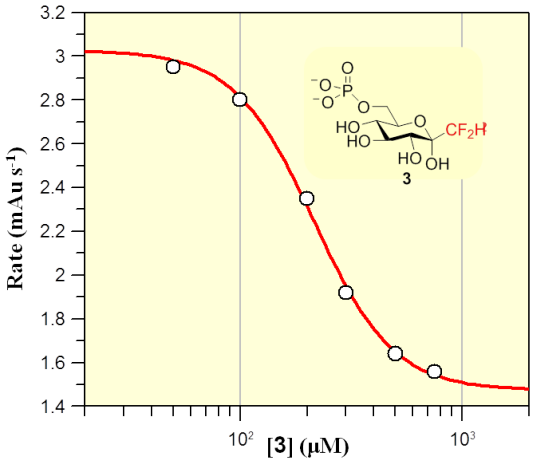

Parameter	Value	Std. Error
Y Range	1.5538	0.0767
IC 50	214.0778	10.9251
Slope factor	2.4233	0.2937
Background	1.4729	0.0591

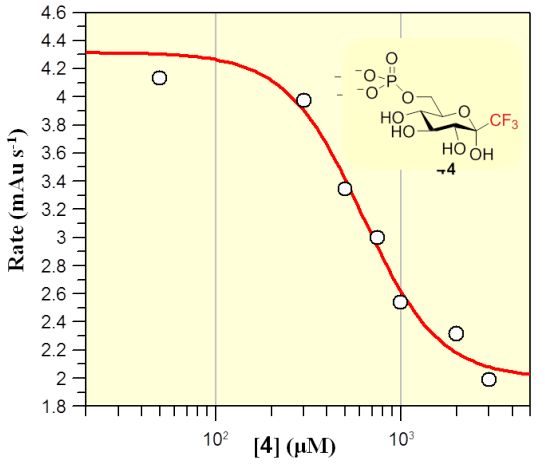

Parameter	Value	Std. Error
Y Range	2.3144	0.2389
IC 50	620.5964	81.8212
Slope factor	2.1038	0.5574
Background	1.9998	0.1914

Figure S5. Sequence alignment of *Xanthomonas citri* PGM (top) and *P. aeruginosa* PMM/PGM (bottom).

Secondary structure for XcPGM is indicated above the alignment. Figure made with ESPript.[3] Key active site regions are highlighted, as described before.[4]

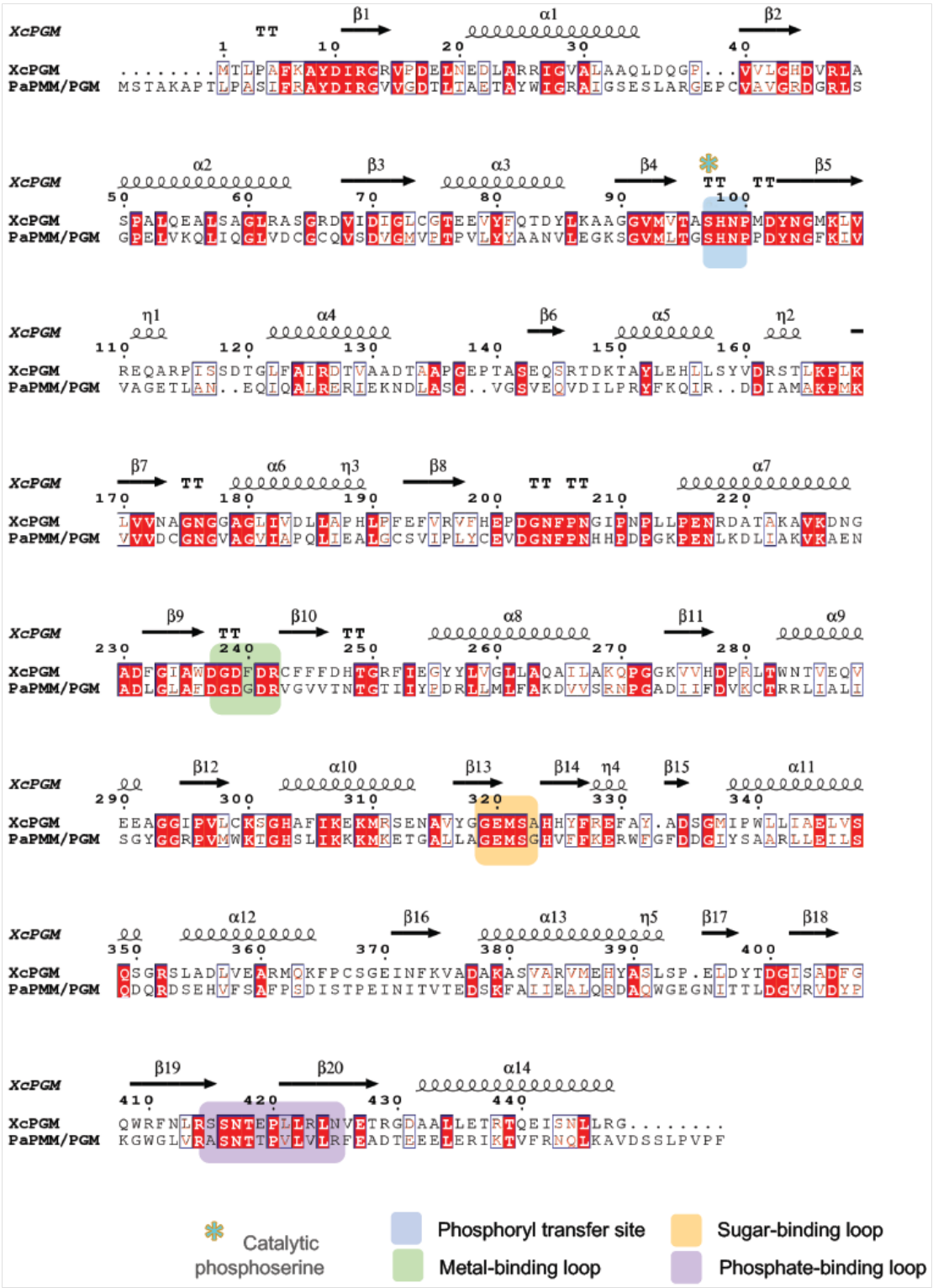

Table S1. X-ray data collection and refinement statistics for the CH3G6P complex. (Statistics for the highest-resolution shell are shown in parentheses.)

Compound #	1

Ligand abbrev.	CH3G6P
PDB ID code	6N1E
Resolution range	38.98 - 1.7 (1.761 - 1.7)
Space group	P 21 21 21
Unit cell	43.705 54.745 172.432 90 90 90
Total reflections	326911 (31655)
Unique reflections	46426 (4571)
Multiplicity	7.0 (6.9)
Completeness (%)	99.59 (99.05)
Mean I/sigma(I)	21.28 (1.59)
Wilson B-factor	21.22
R-merge	0.07415 (1.23)
R-meas	0.08007 (1.328)
R-pim	0.02991 (0.4985)
CC1/2	0.999 (0.634)
Reflections used in refinement	46386 (4571)
R-work	0.1635 (0.2323)
R-free	0.2019 (0.2658)
Number of non-hydrogen atoms	4050
macromolecules	3499
ligands	17
solvent	533

Protein residues	448
RMS(bonds)	0.008
RMS(angles)	1.21
Ramachandran favored (%)	97.09
Ramachandran allowed (%)	2.69
Ramachandran outliers (%)	0.22
Clashscore	0.27
Average B-factor	3.88
macromolecules	26.21
ligands	24.61
solvent	43.18

Table S2. A comparison of protein-ligand hydrogen bonds of complex between the 1-XcPGM and αG1P.

Ligand atom	**Protein residue & atom** [a]	**αG1P (5BMP)**	**1**
Phosphate contacts (Å)			
O1P	R414 NH1	3.04	2.87
	R423 NE	2.87	3.44
O2P	R414 NH2	2.67	2.75
	N417 N	2.83	3.15
O3P	S416 OG	2.53	2.58
	T418 OG1	2.52	2.82
	R423 NH1	3.04	3.48
Sugar hydroxyl contacts (Å)			

O2	R280 NH1	2.55	- [b]
O3	R280 NH2	2.97	-
	H303 N	-	2.99
	E320 OE2	2.59	2.75
	S322 OG	2.61	-
O4	H303 N	3.14	-
	E320 OE1	2.84	3.31

[a] residue numbers correspond to the XcPGM sequence from UniProt ID Q8PGN7 (without His tag). [b] corresponding interaction is missing.

^{1}H, ^{13}C, ^{19}F, and ^{31}P NMR spectra of synthetic intermediates and final products

Figure S6. ^{1}H NMR (300 MHz, $CDCl_3$) spectra of compound 9

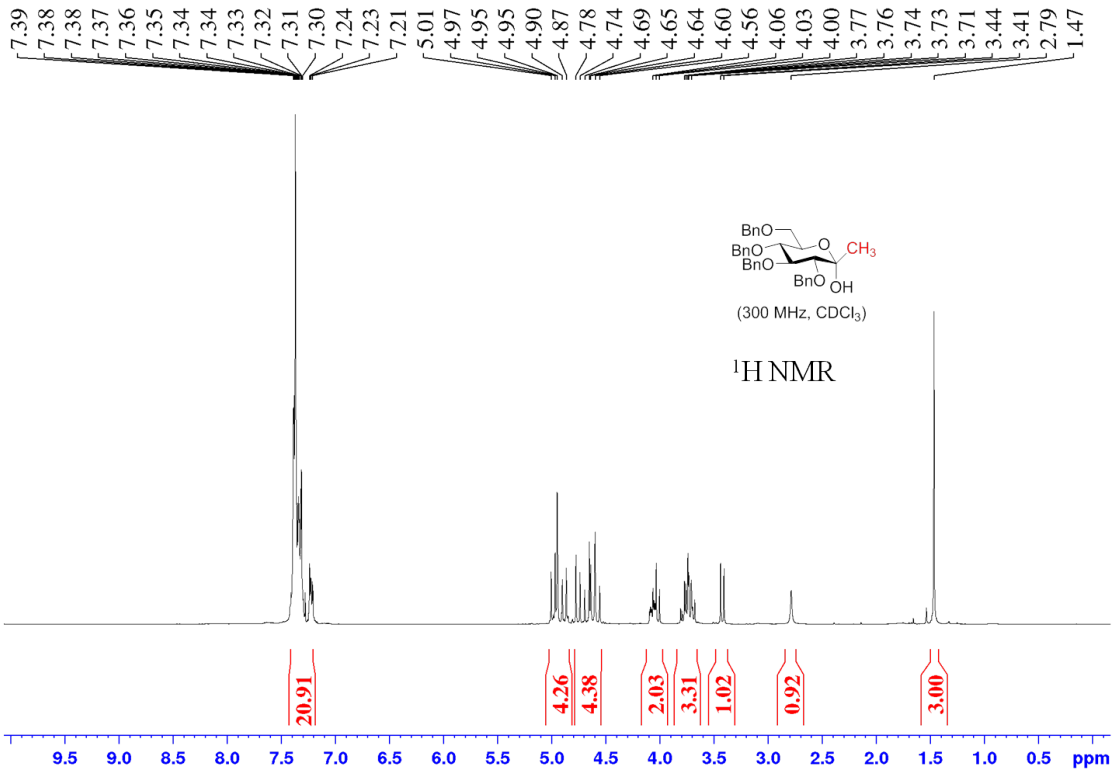

Figure S7. ^{1}H NMR (500 MHz, D_2O) spectra of compound 12

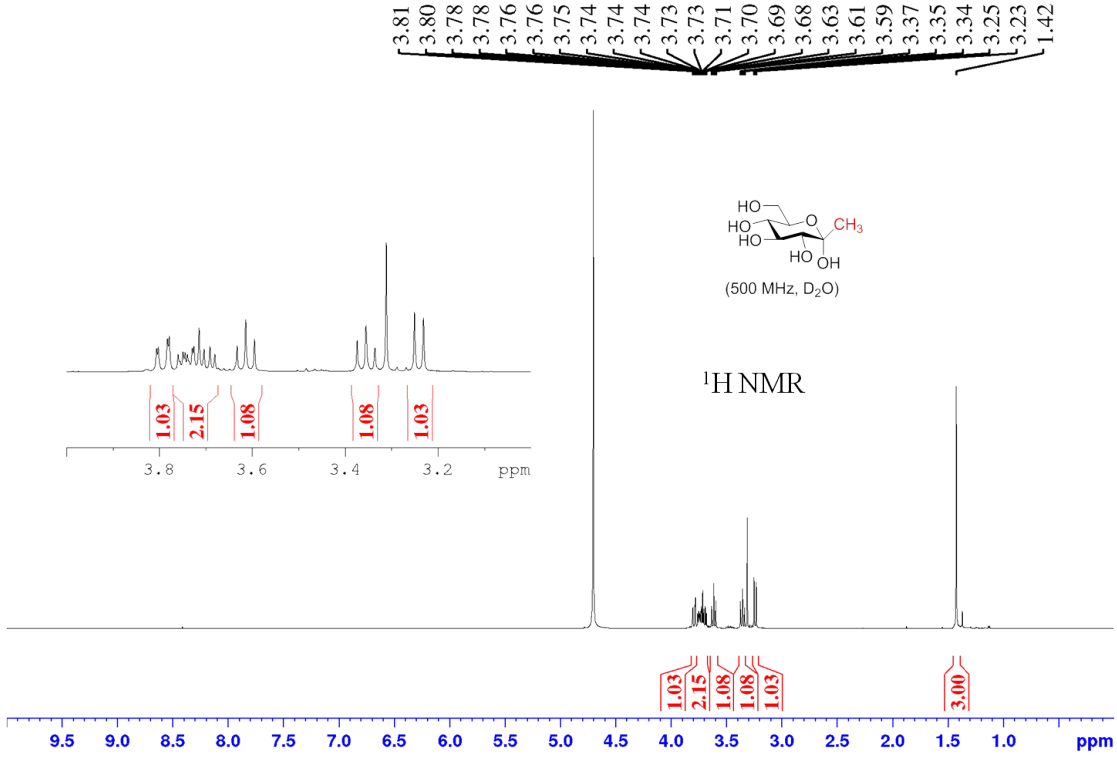

Figure S8. ^{13}C NMR (125 MHz, D_2O) spectra of compound 12

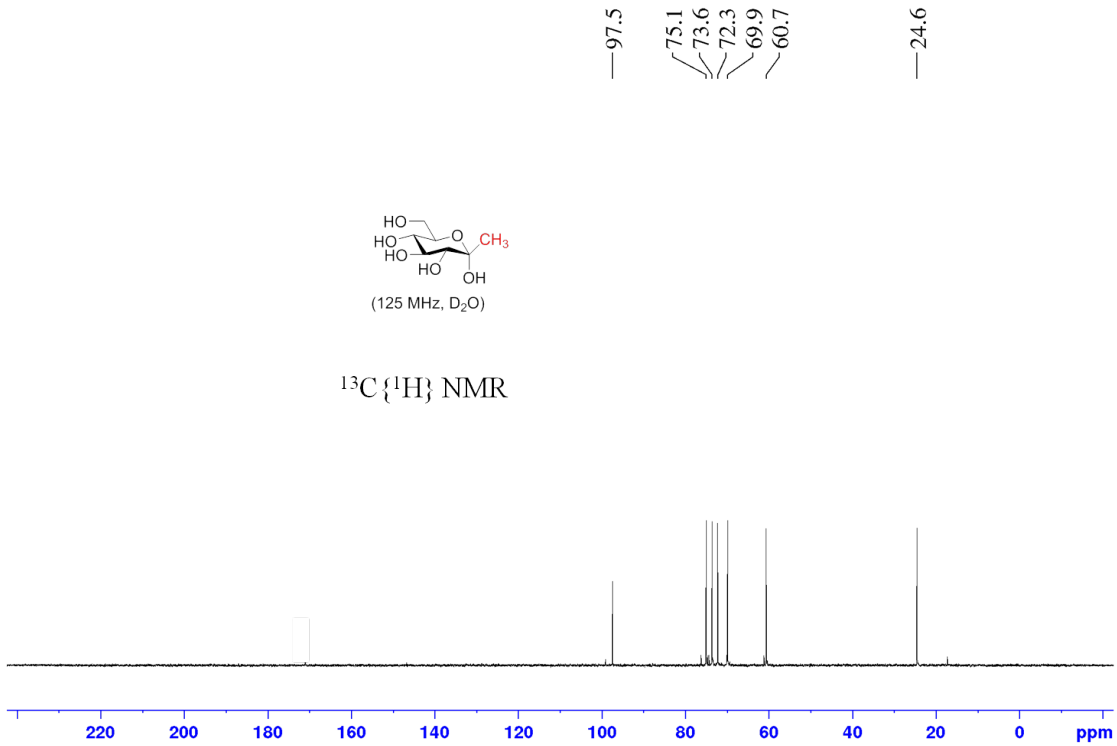

Figure S9. ^{1}H NMR (500 MHz, D_2O) spectra of compound 1

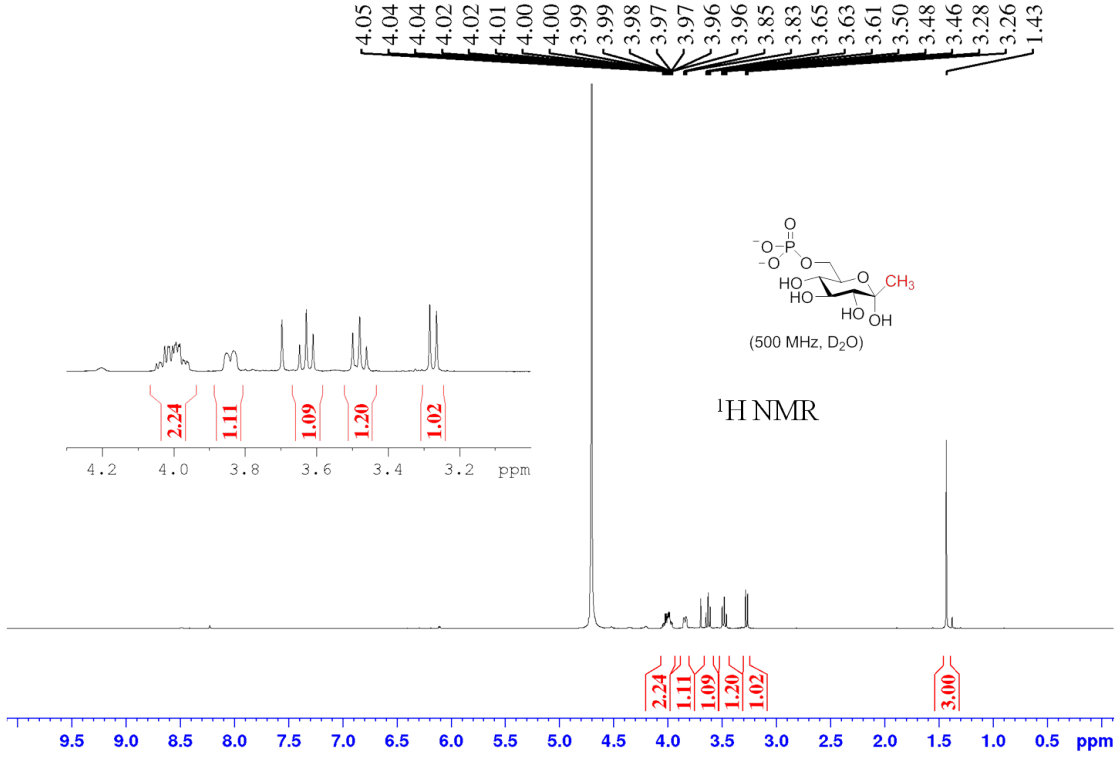

Figure S10. ^{31}P NMR (202 MHz, D_2O) spectra of compound 1

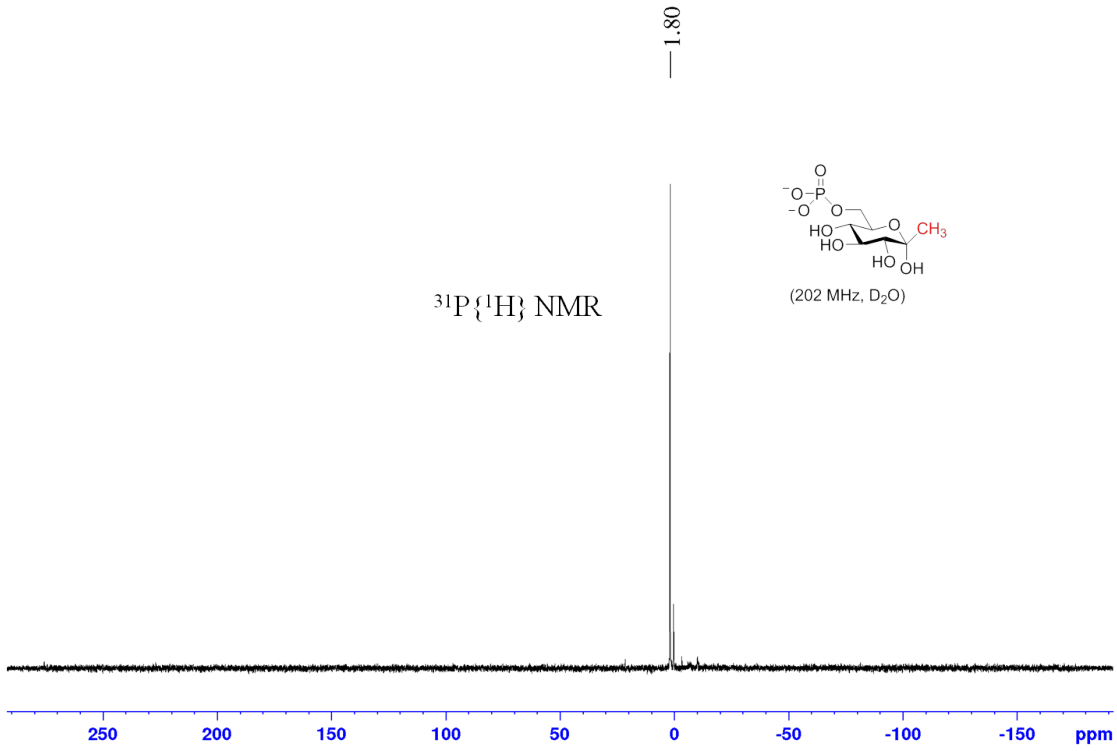

Figure S11. ^{13}C NMR (125 MHz, D_2O) spectra of compound 1

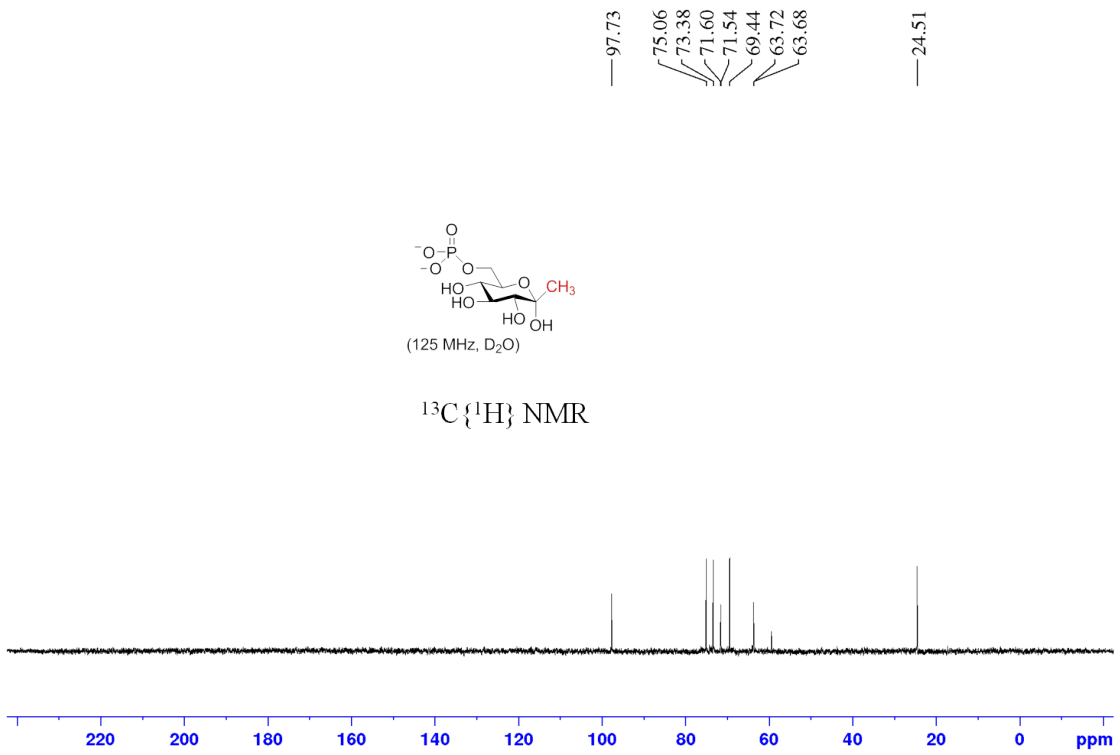

Figure S12. ^{19}F NMR (470 MHz, DMSO-d^6) spectra of compound 10

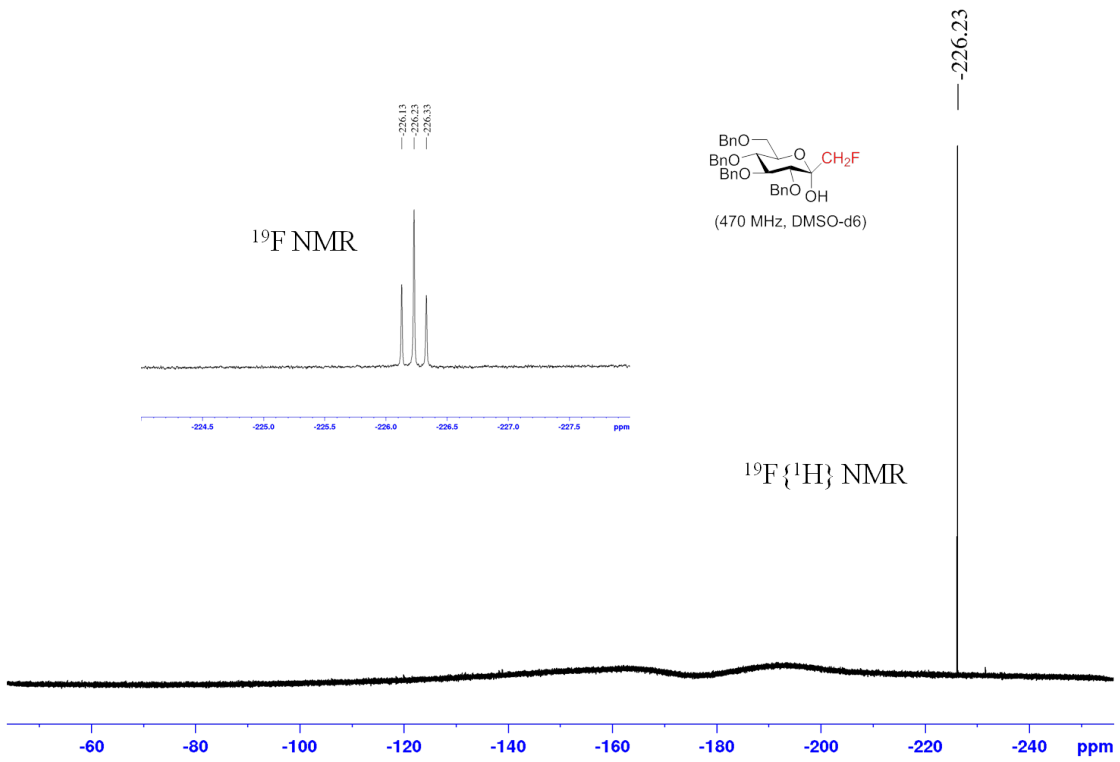

Figure S13. ^{19}F NMR (470 MHz, D_2O) spectra of compound 13

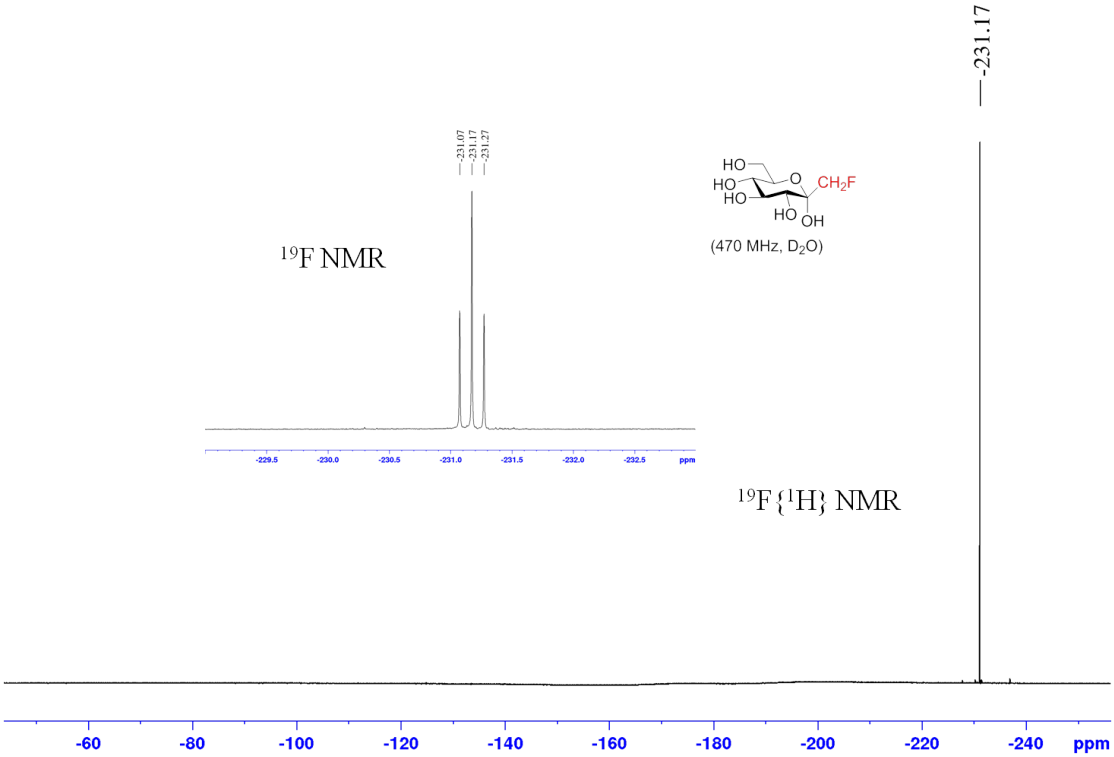

Figure S14. ^{1}H NMR (500 MHz, D_2O) spectra of compound 2

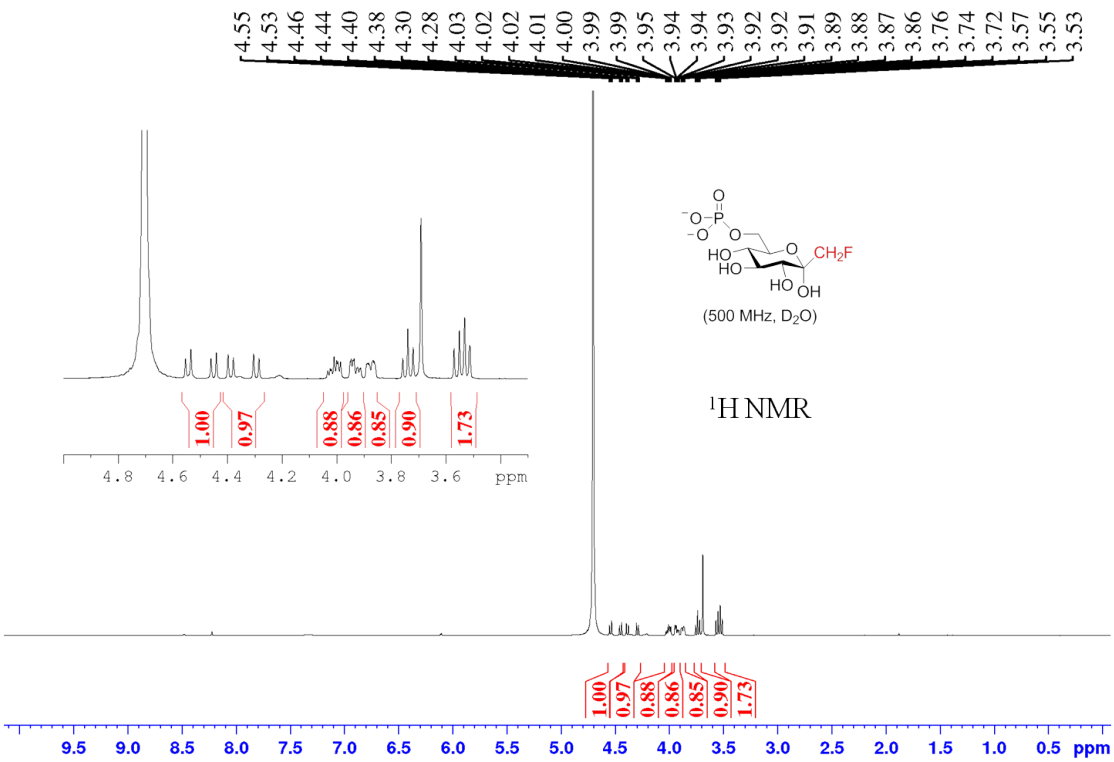

Figure S15. ^{19}F NMR (470 MHz, D_2O) spectra of compound 2

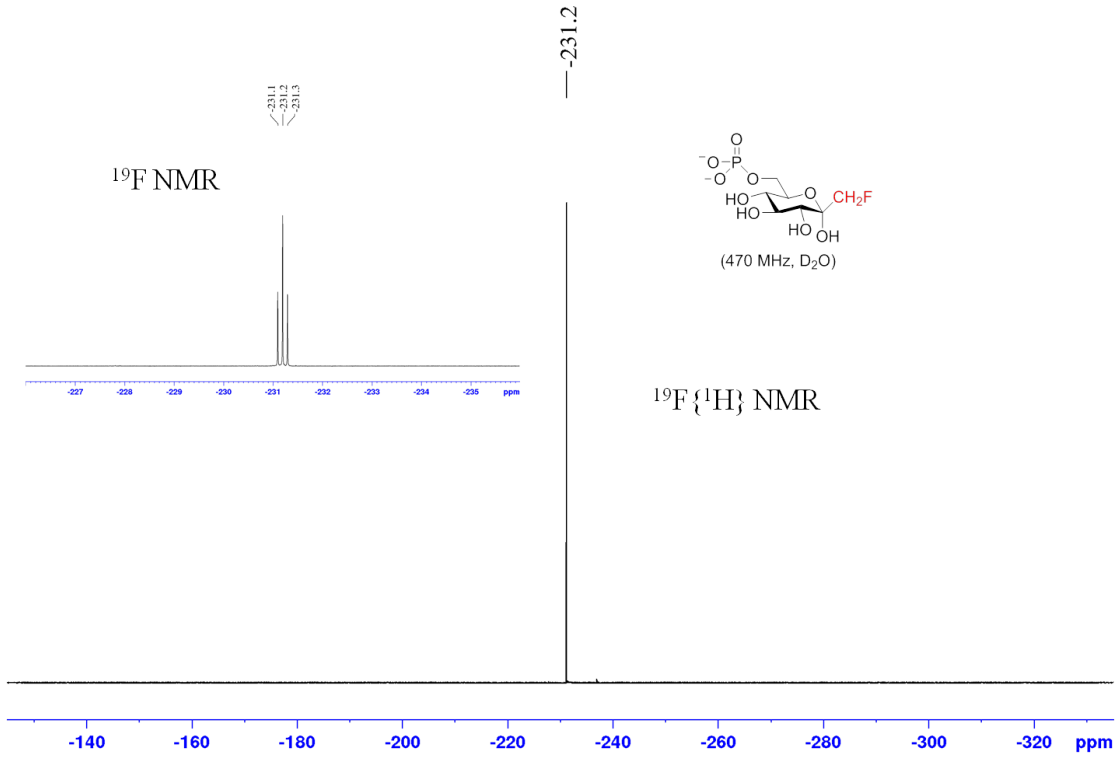

Figure S16. ^{31}P NMR (202 MHz, D_2O) spectra of compound 2

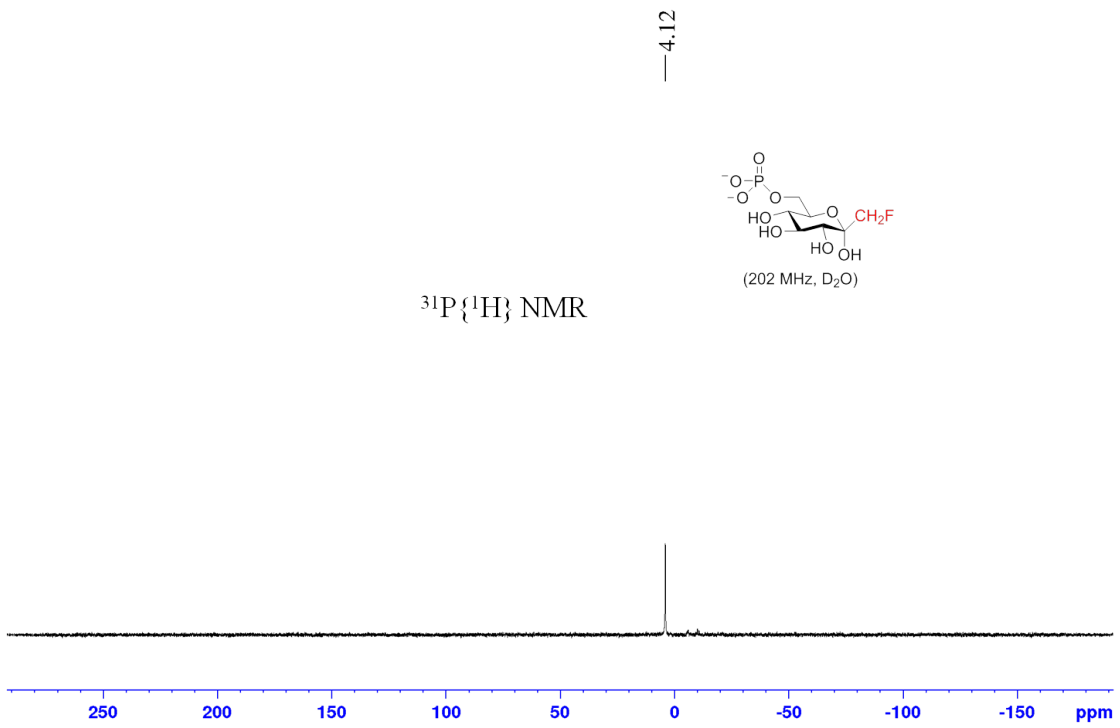

Figure S17. ^{13}C NMR (125 MHz, D_2O) spectra of compound 2

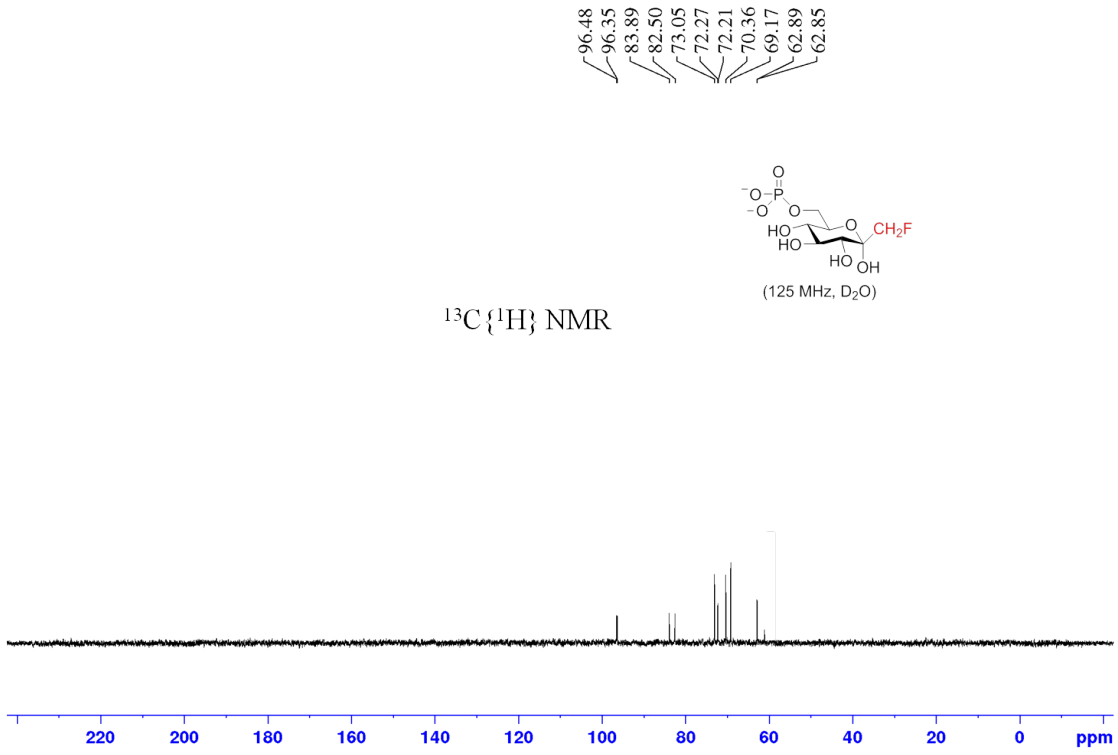

Figure S18. ^{1}H NMR (500 MHz, $CDCl_3$) spectra of compound 6

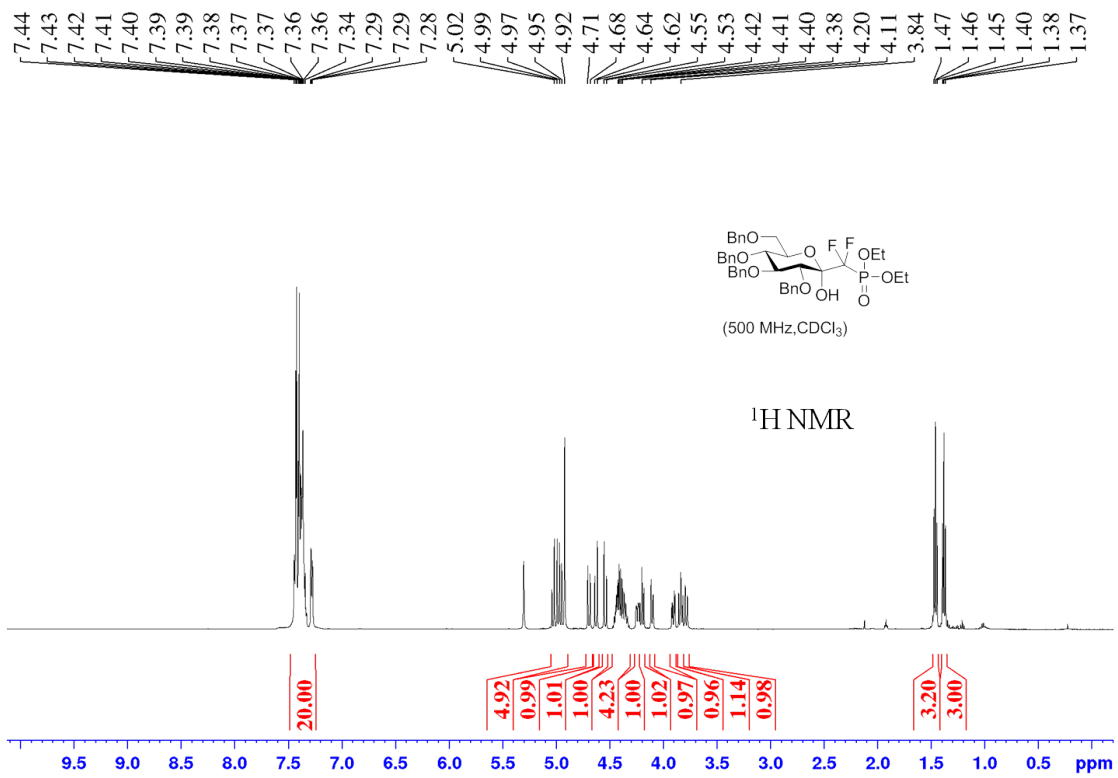

Figure S19. ^{19}F NMR (470 MHz, $CDCl_3$) spectra of compound 6

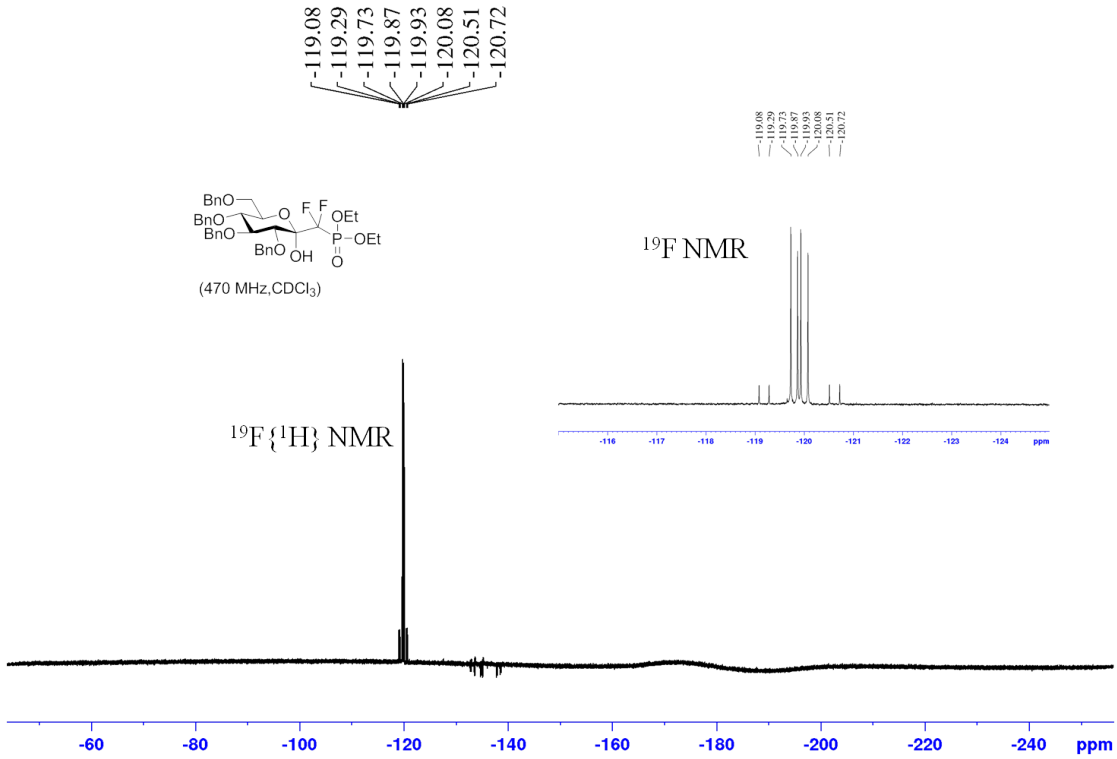

Figure S20. ^{31}P NMR (202 MHz, $CDCl_3$) spectra of compound 6

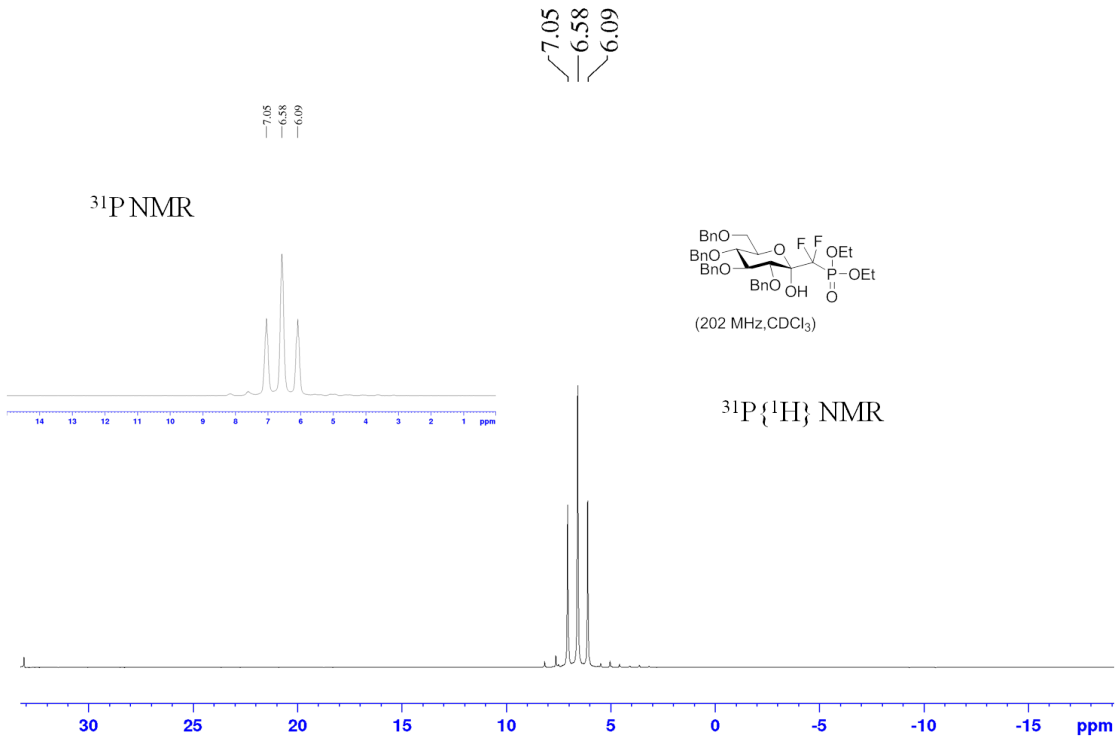

Figure S21. ^{1}H NMR (500 MHz, $CDCl_3$) spectra of compound 7

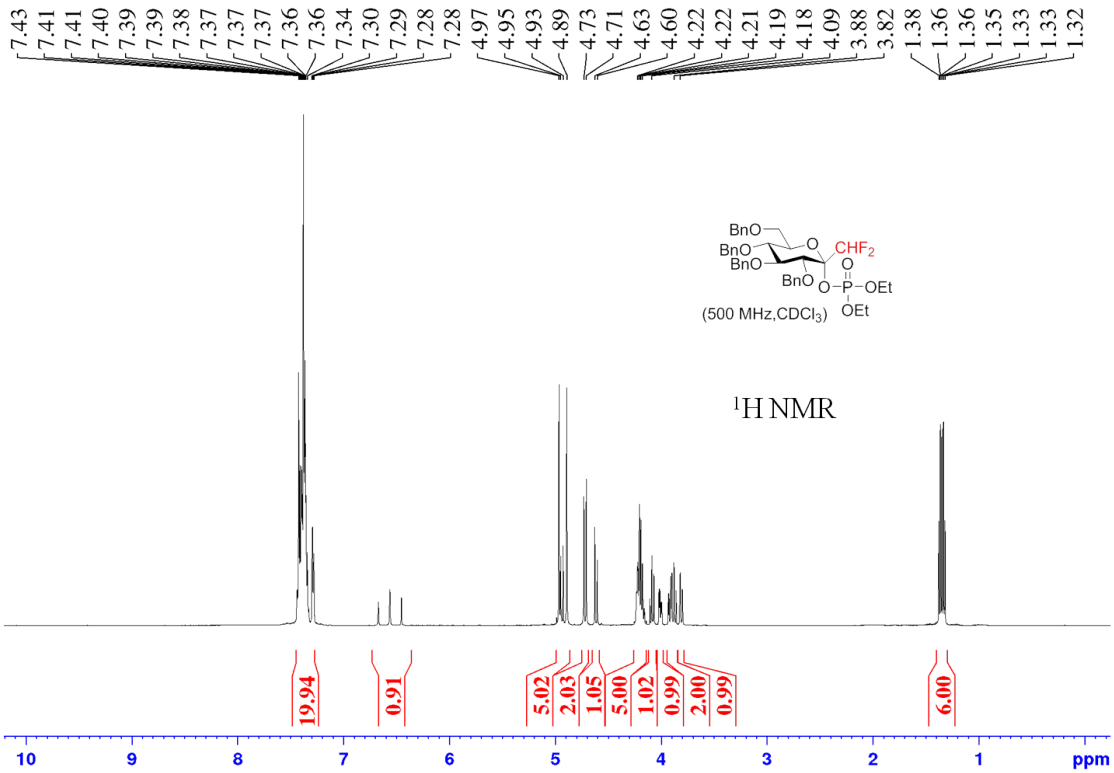

Figure S22. ^{19}F NMR (470 MHz, $CDCl_3$) spectra of compound 7

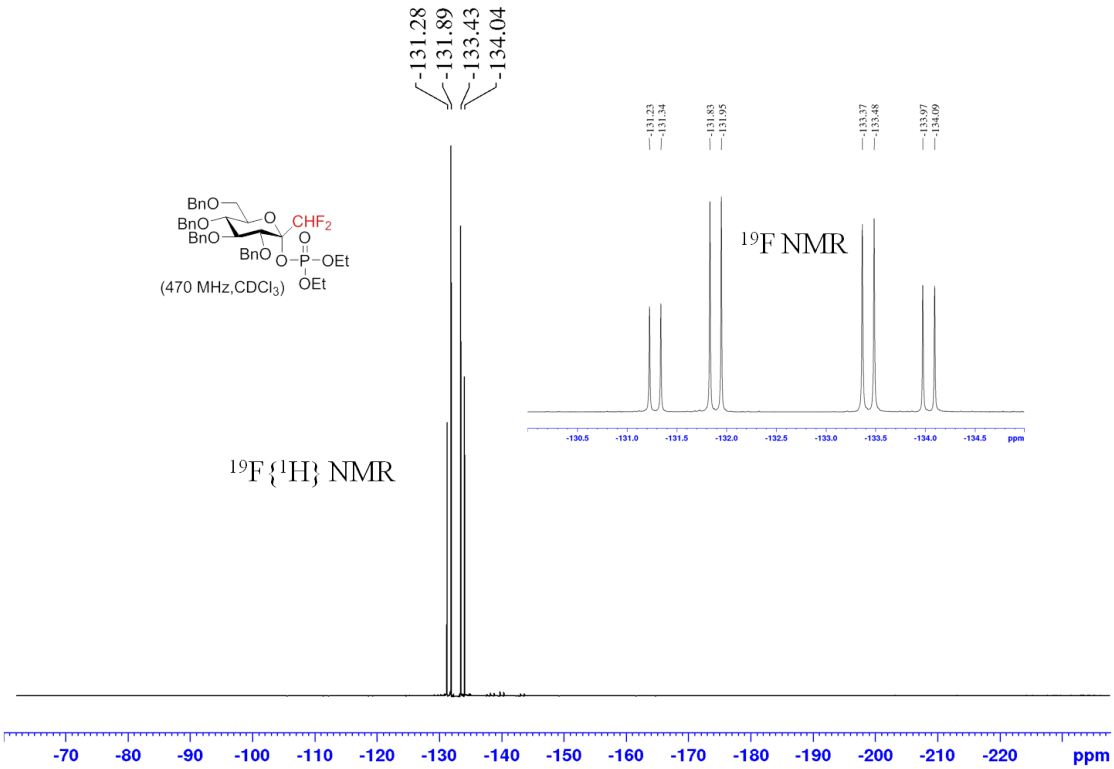

Figure S23. ^{31}P NMR (202 MHz, $CDCl_3$) spectra of compound 7

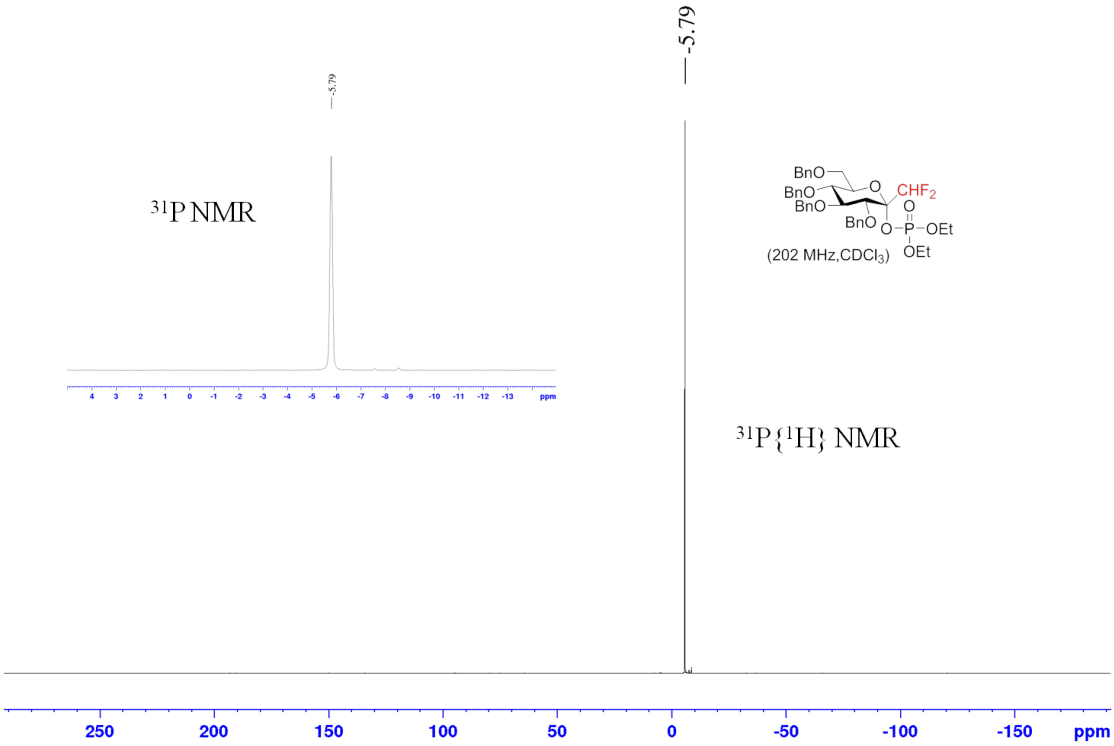

Figure S24. ^{13}C NMR (125 MHz, $CDCl_3$) spectra of compound 7

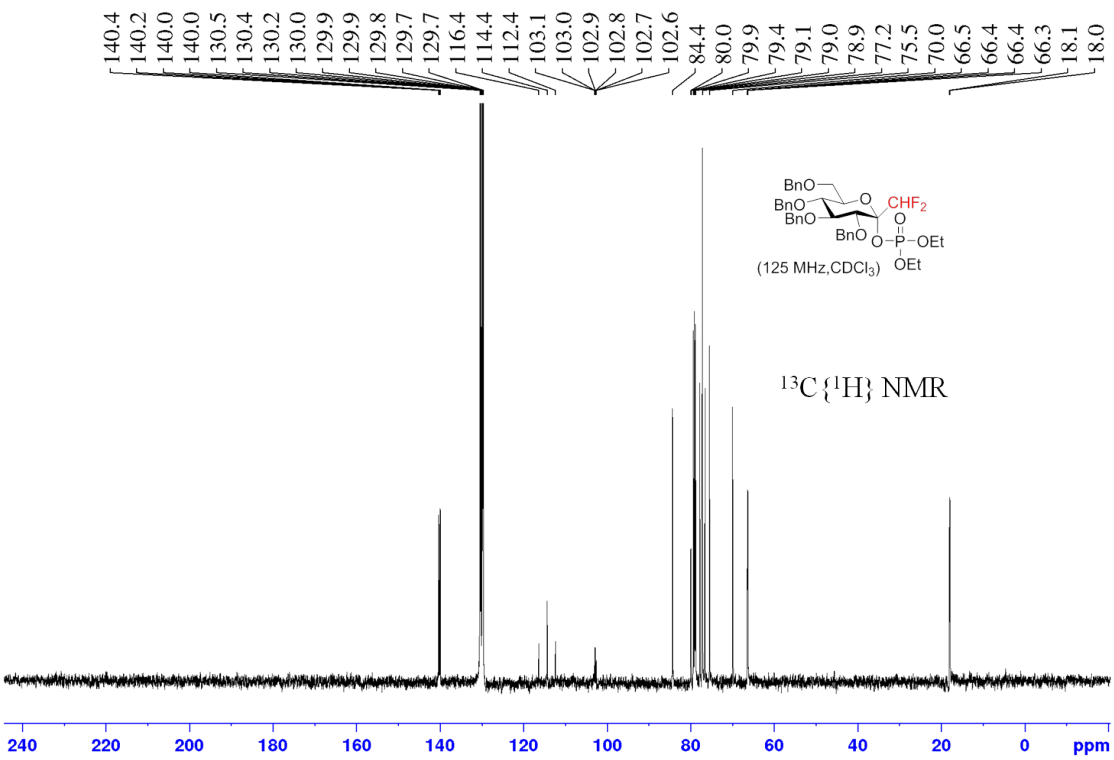

Figure S25. ^{1}H NMR (500 MHz, $CDCl_3$) spectra of compound 8

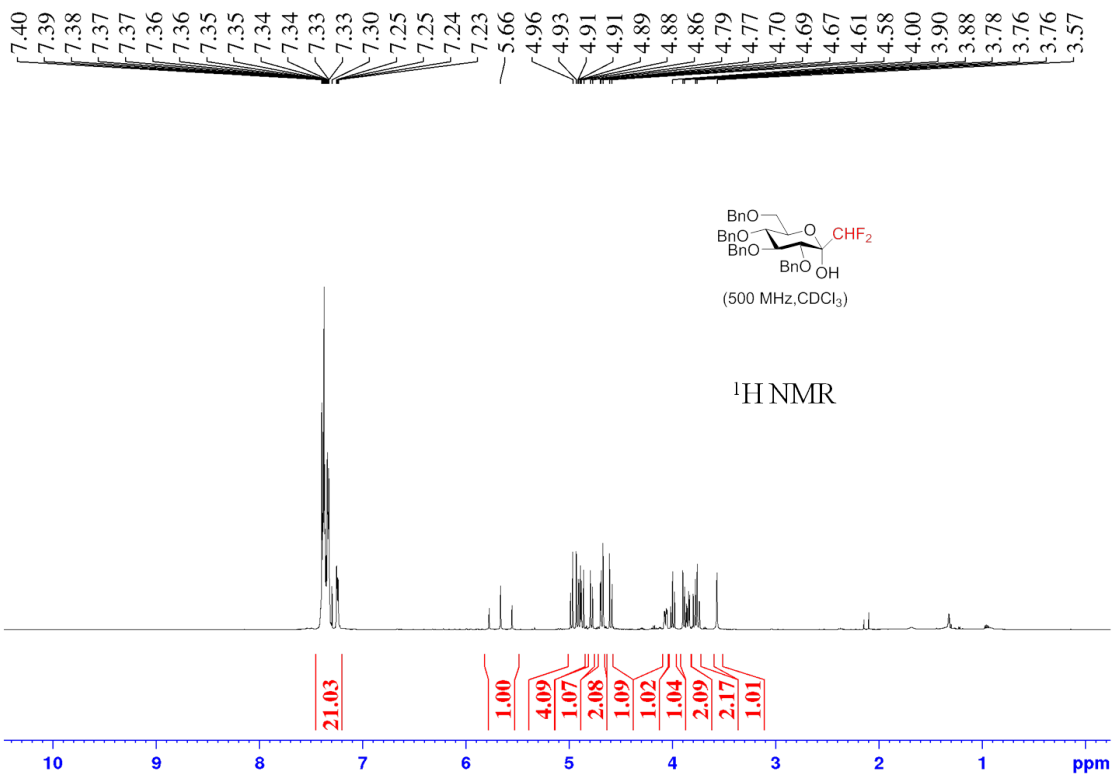

Figure S26. ^{19}F NMR (470 MHz, $CDCl_3$) spectra of compound 8

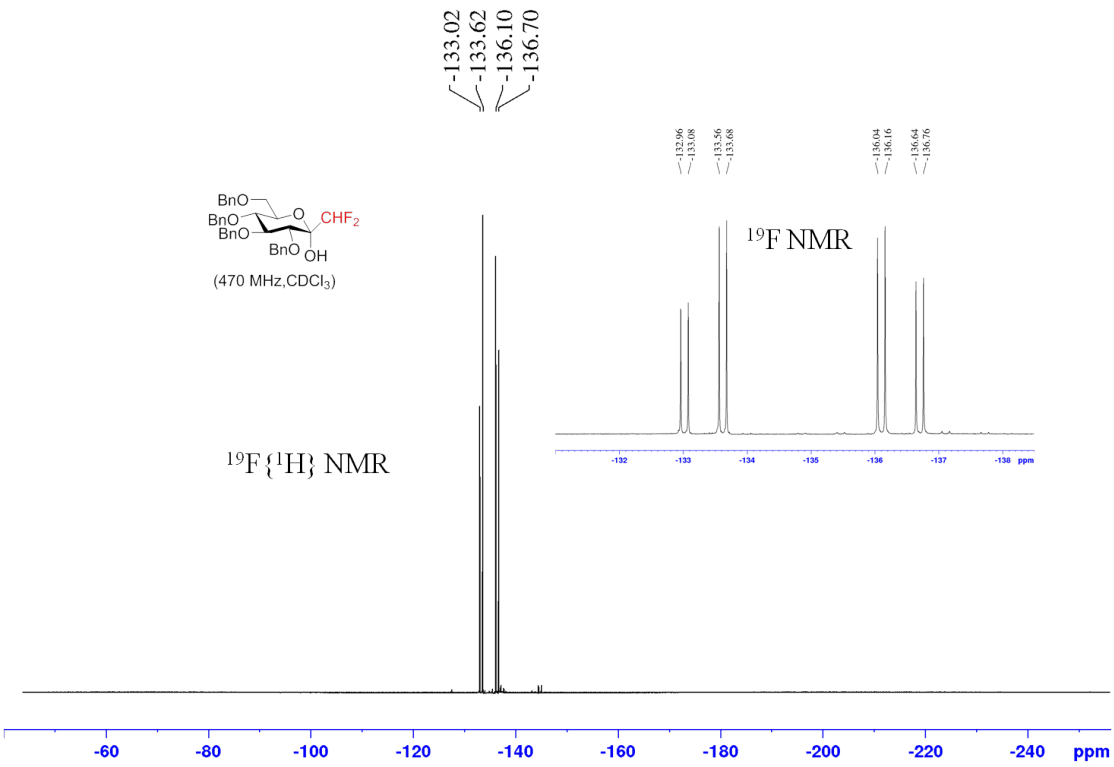

Figure S27. ^{1}H NMR (500 MHz, D_2O) spectra of compound 14

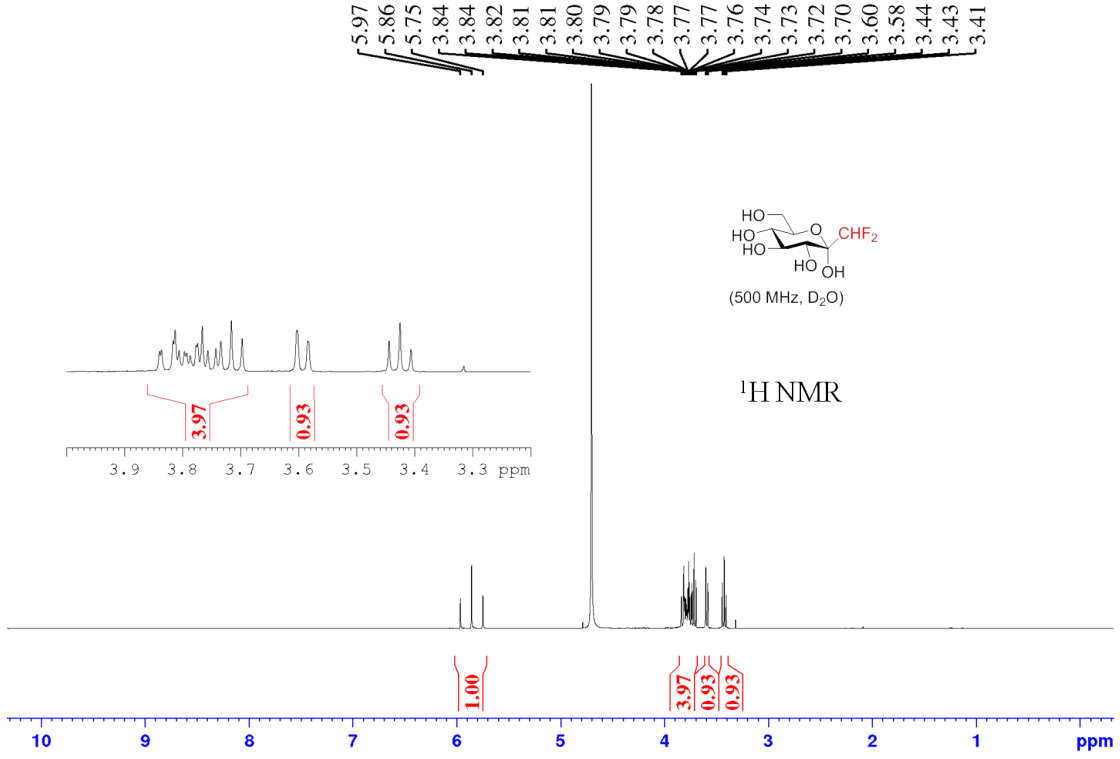

Figure S28. ^{19}F NMR (470 MHz, D_2O) spectra of compound 14

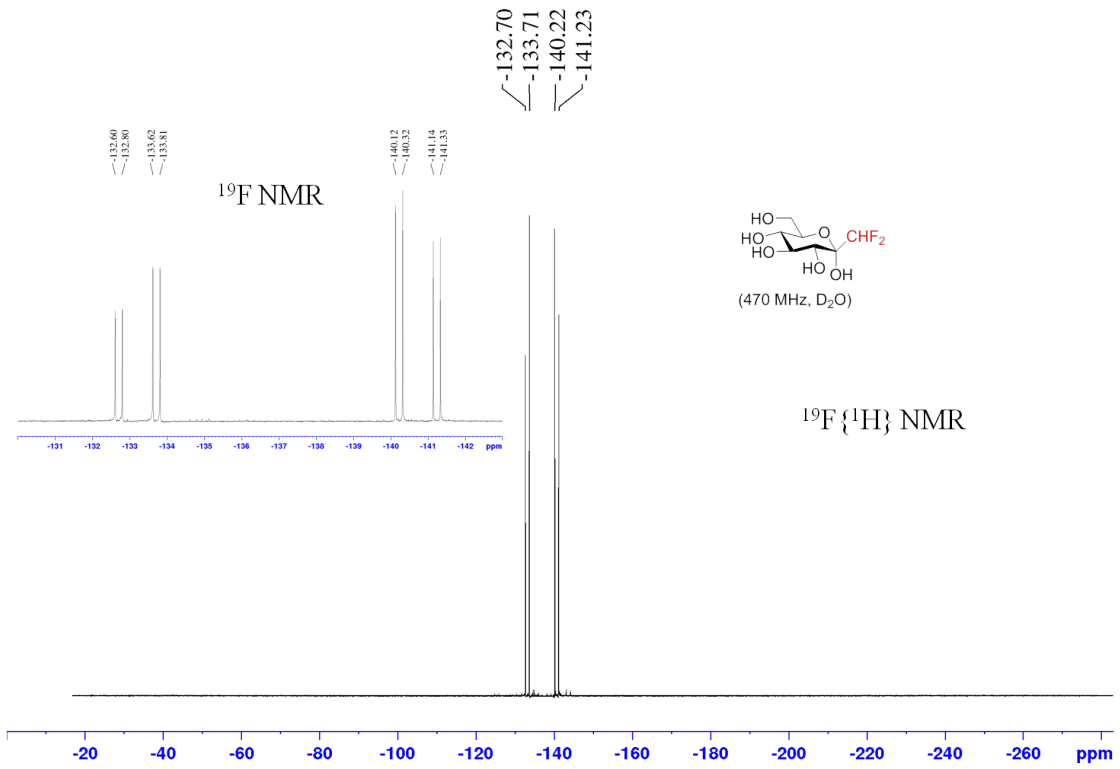

Figure S29. ^{13}C NMR (125 MHz, D_2O) spectra of compound 14

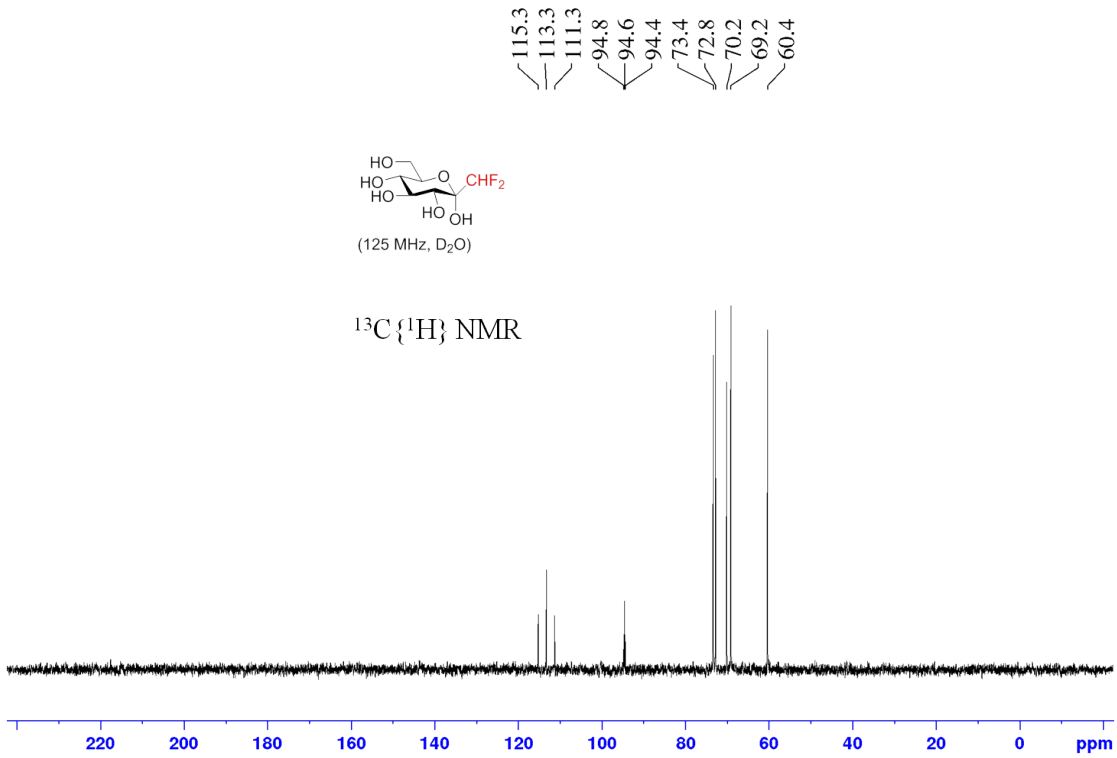

Figure S30. ^{1}H NMR (500 MHz, D_2O) spectra of compound 3

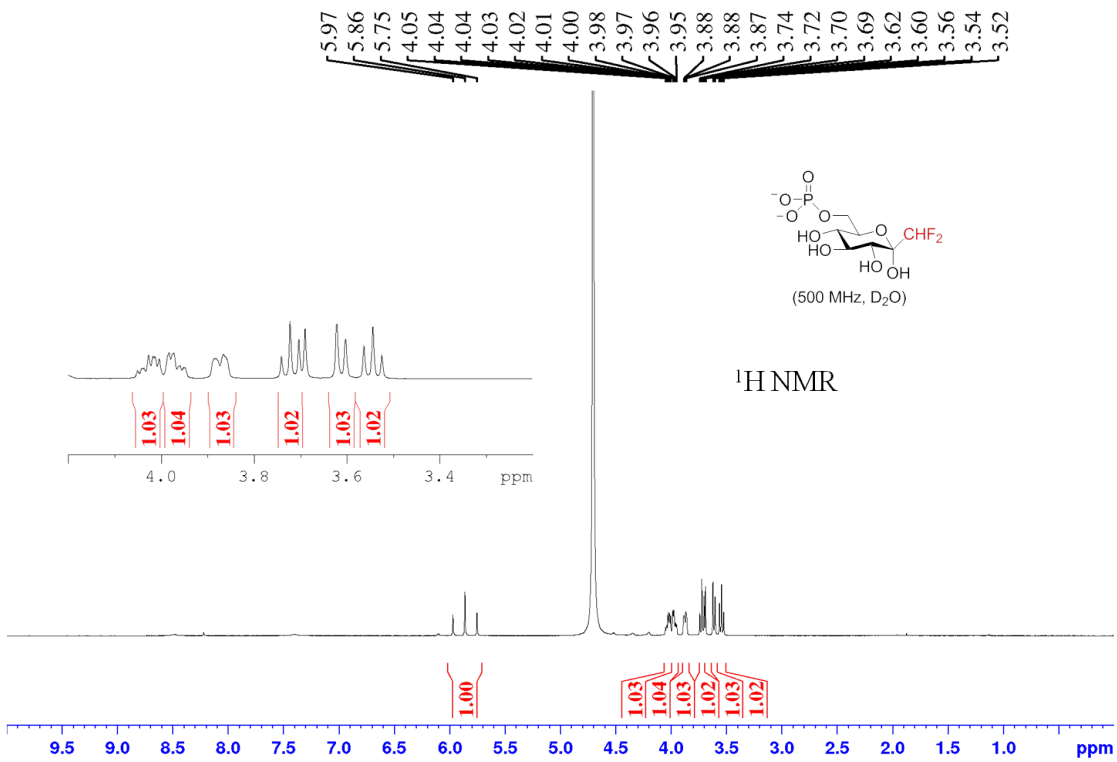

Figure S31. ^{19}F NMR (470 MHz, D_2O) spectra of compound 3

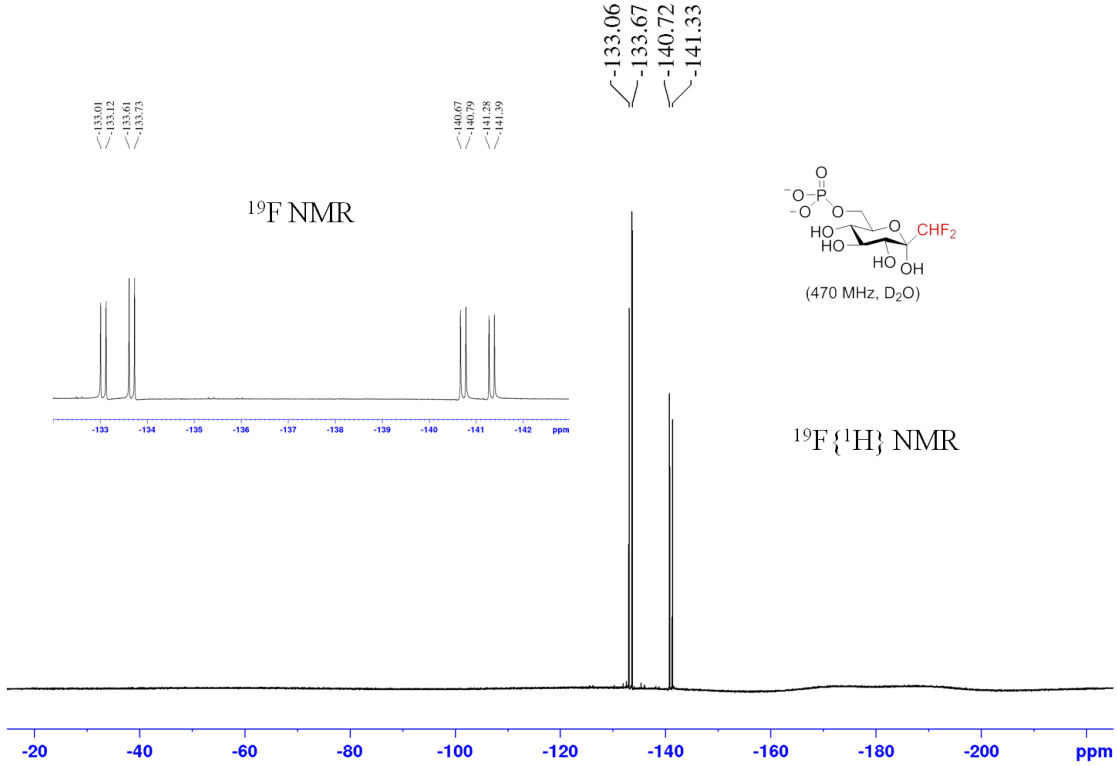

Figure S32. ^{31}P NMR (202 MHz, D_2O) spectra of compound 3

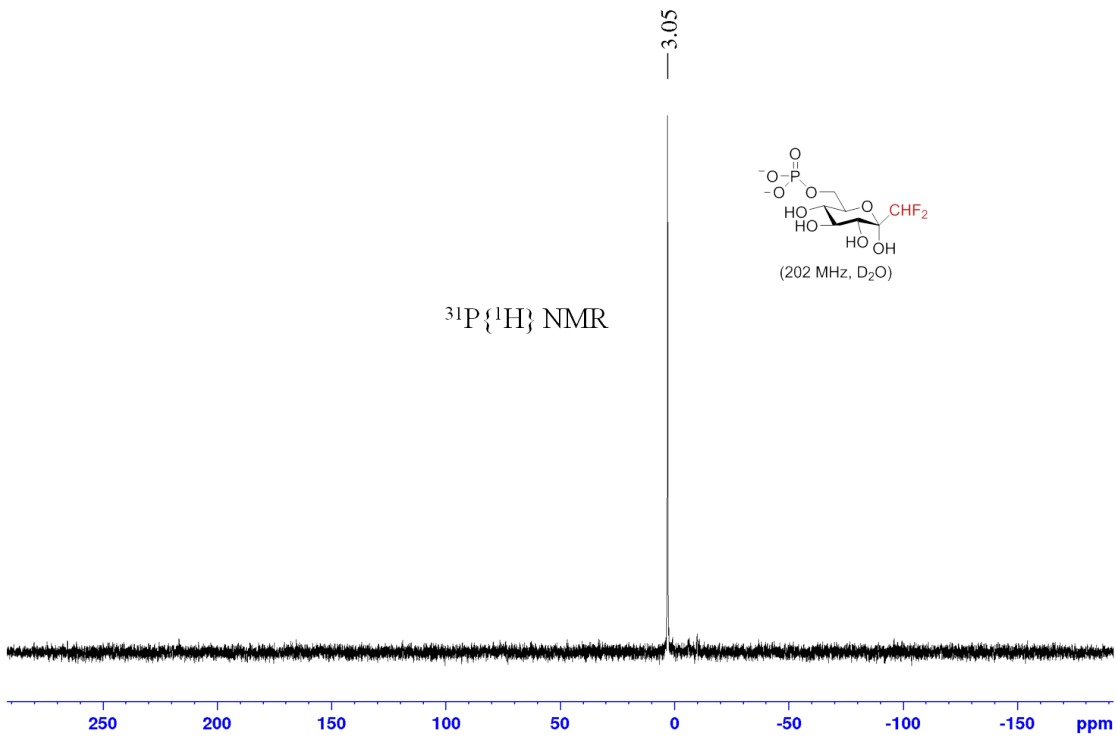

Figure S33. ^{13}C NMR (125 MHz, D_2O) spectra of compound 3

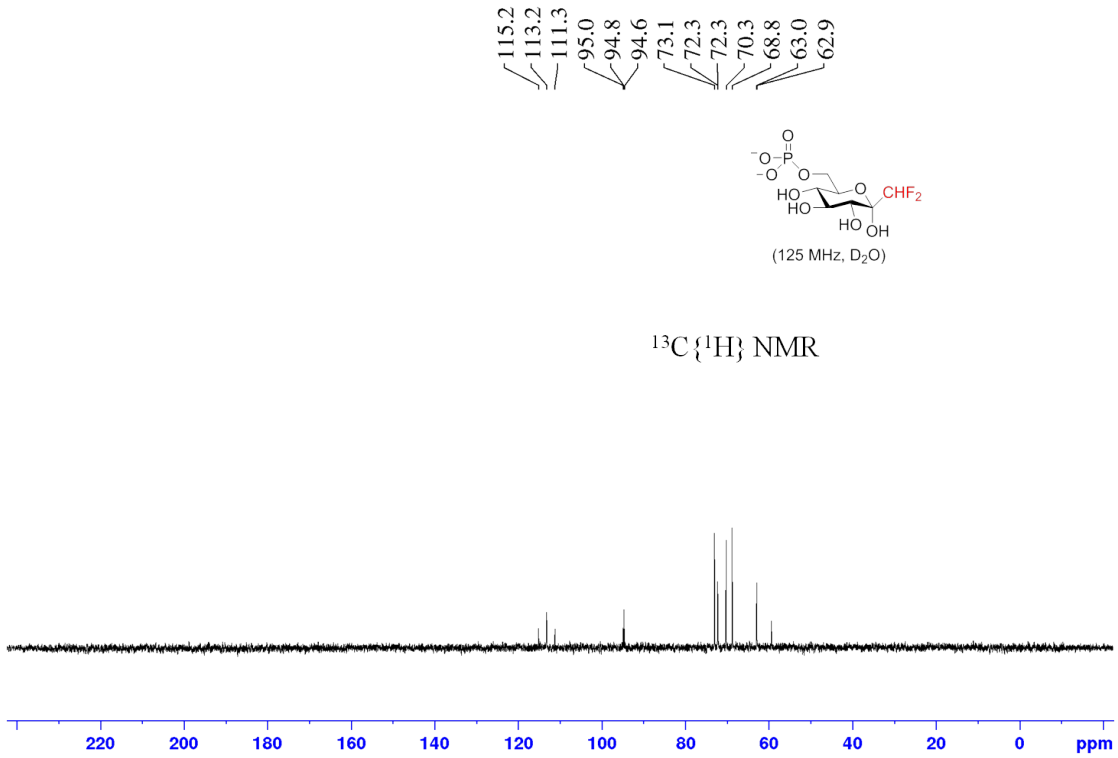

Figure S34. ^{19}F NMR (470 MHz, $CDCl_3$) spectra of compound 11

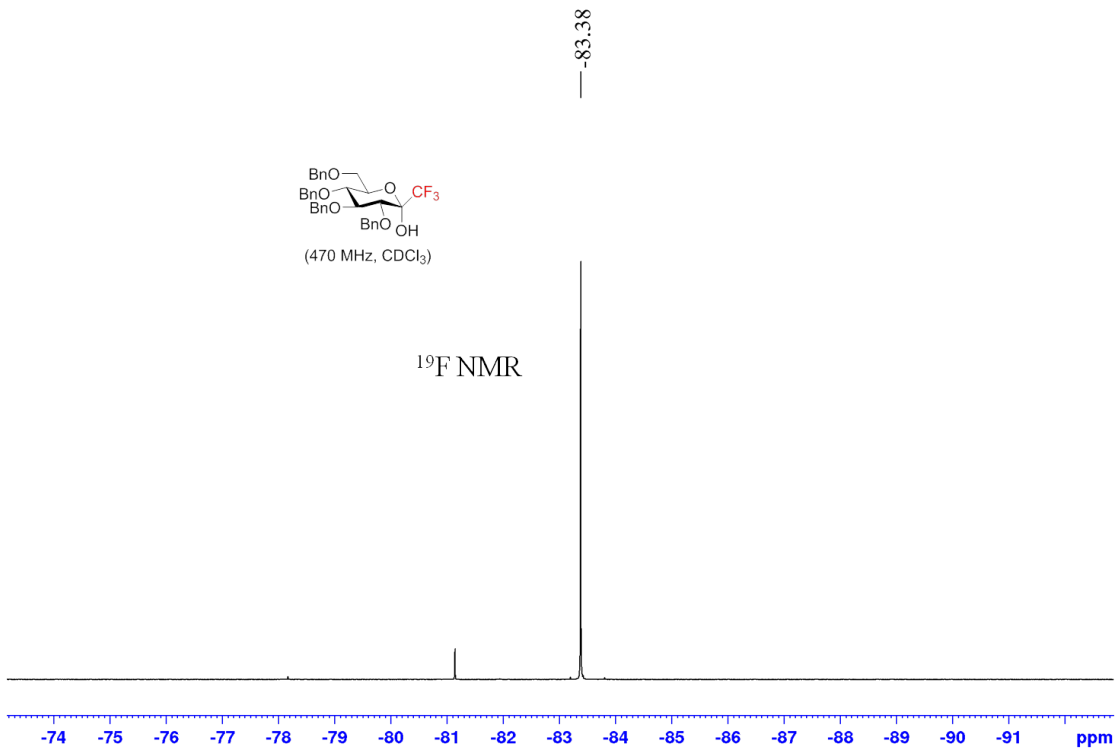

Figure S35. ^{1}H NMR (500 MHz, D_2O) spectra of compound 15

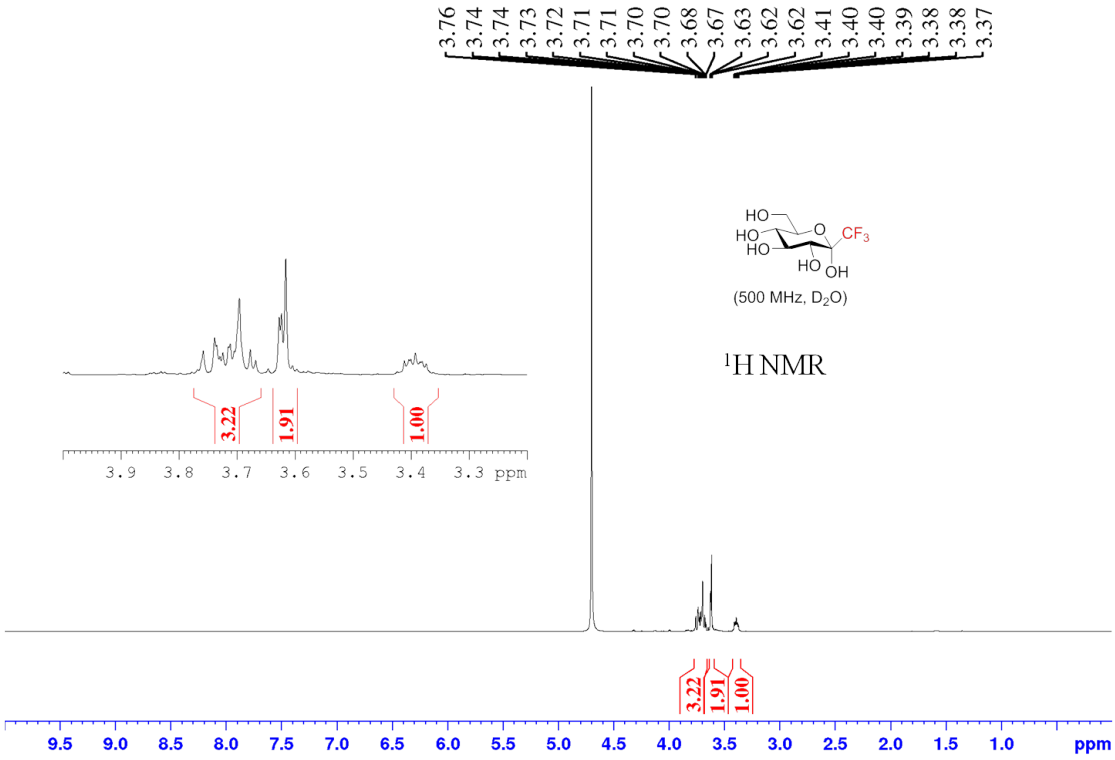

Figure S36. ^{19}F NMR (470 MHz, D_2O) spectra of compound 15

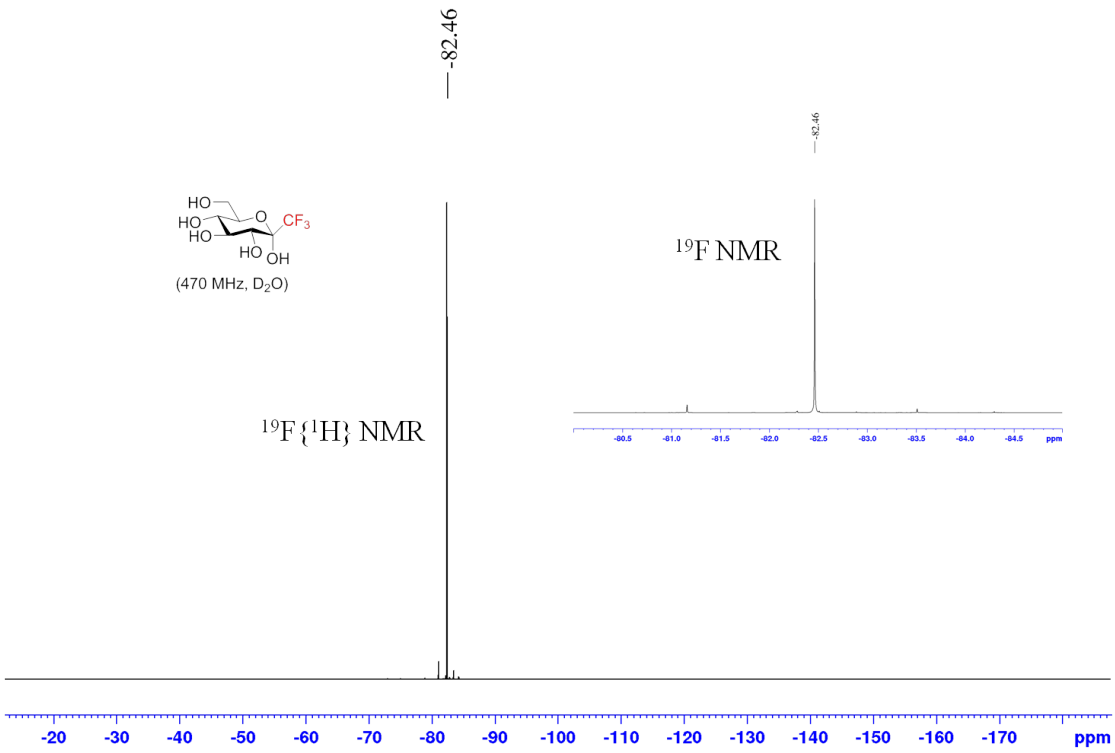

Figure S37. ^{13}C NMR (125 MHz, D_2O) spectra of compound 15

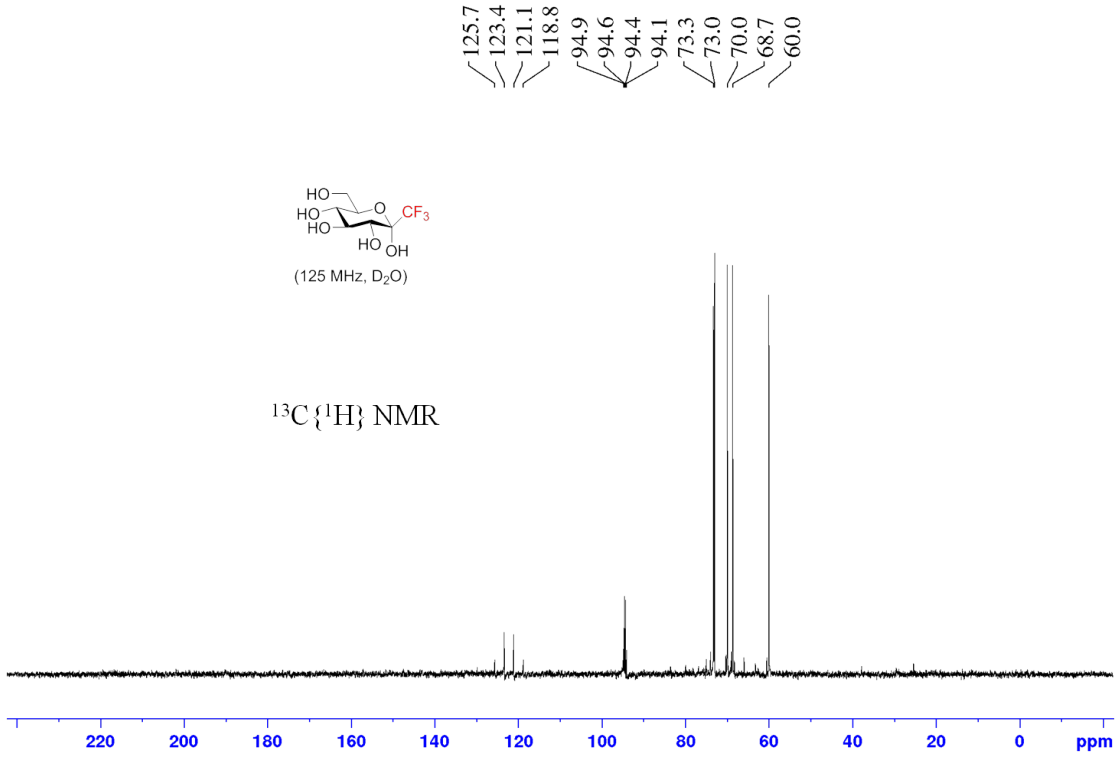

Figure S38. ^{1}H NMR (500 MHz, D_2O) spectra of compound 4

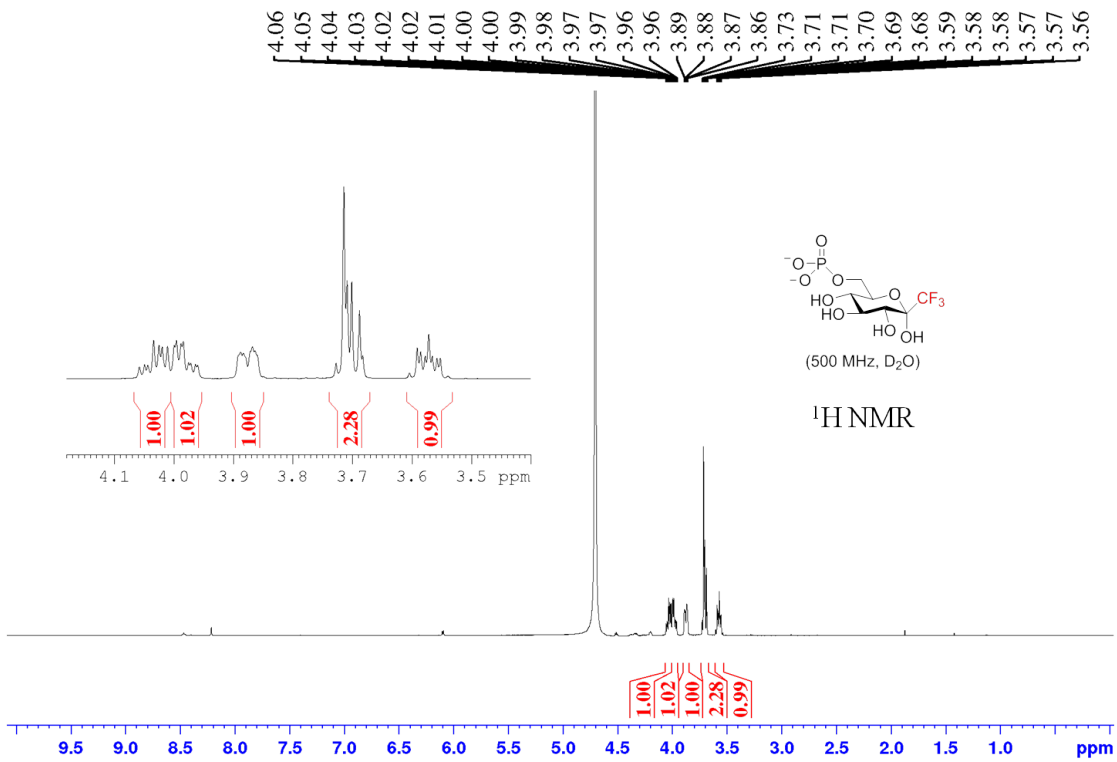

Figure S39. ^{19}F NMR (470 MHz, D_2O) spectra of compound 4

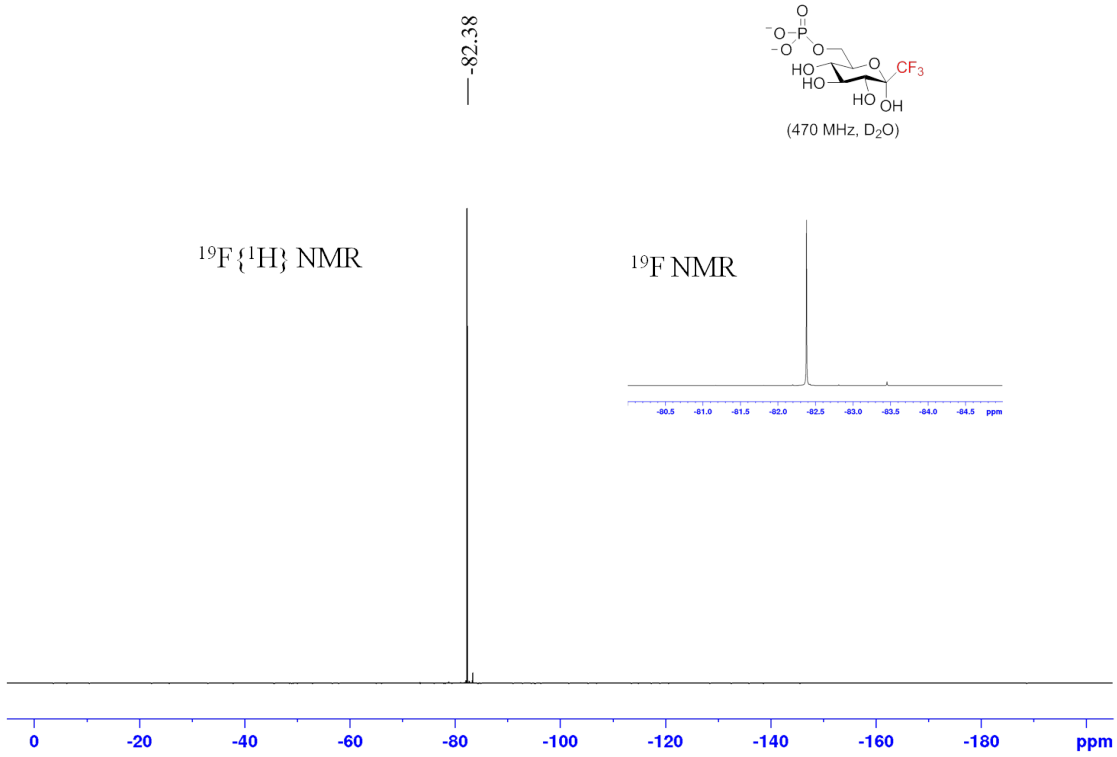

Figure S40. ^{31}P NMR (202 MHz, D_2O) spectra of compound 4

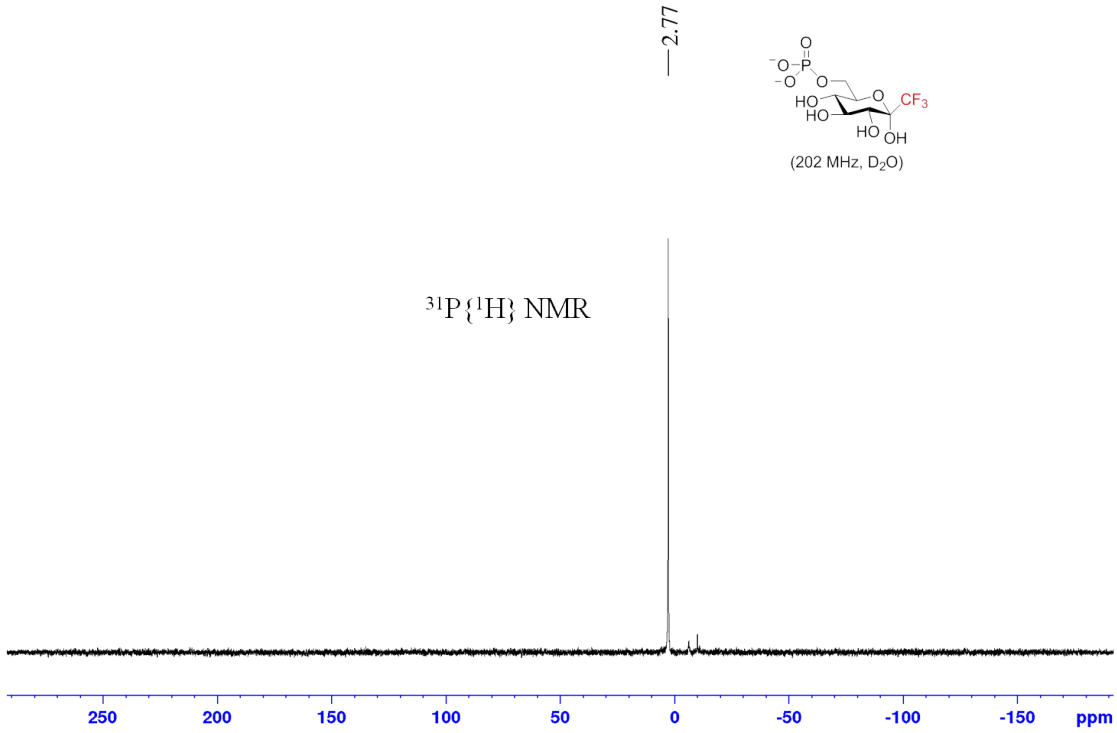

Figure S41. ^{13}C NMR (125 MHz, D_2O) spectra of compound 4

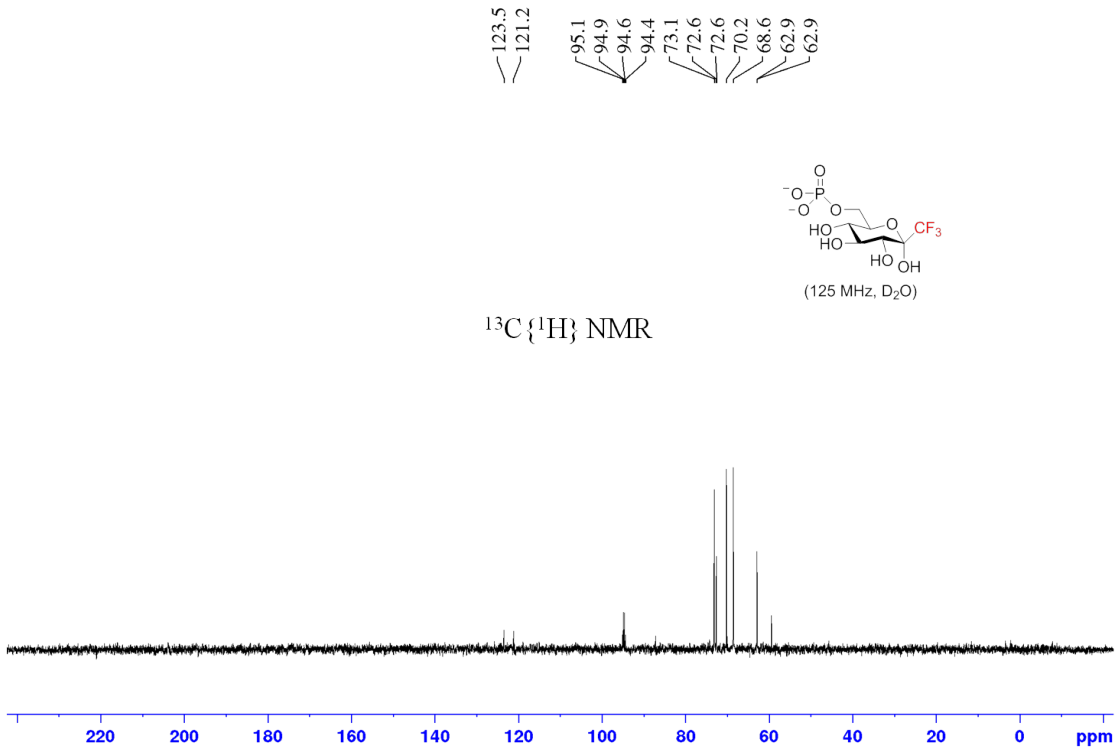

References

(1) Schramm, A. M.; Mehra-Chaudhary, R.; Furdui, C. M.; Beamer, L. J. Backbone Flexibility, Conformational Change, and Catalysis in a Phosphohexomutase from Pseudomonas aeruginosa. *Biochemistry* **2008**, *47*, 9154-9162.

(2) (a) Zhang, G.; Dai, J.; Wang, L.; Dunaway-Mariano, D.; Tremblay, L. W.; Allen, K. N. Catalytic Cycling in β-Phosphoglucomutase: A Kinetic and Structural Analysis. *Biochemistry* **2005**, *44*, 9404-9416; (b) Ampaw, A.; Carroll, M.; von Velsen, J.; Bhattasali, D.; Cohen, A.; Bowler, M.; Jakeman, D. L. Observing enzyme ternary transition state analogue complexes by 19F NMR spectroscopy. *Chem. Sci.* **2017**, *8*, 8427-8434.

(3) Gouet, P.; Robert, X.; Courcelle, E. ESPript/ENDscript: extracting and rendering sequence and 3D information from atomic structures of proteins. *Nucleic Acids Res.* **2003**, *31*, 3320-3323.

(4) Stiers, K. M.; Muenks, A. G.; Beamer, L. J. Biology, Mechanism, and Structure of Enzymes in the α-d-Phosphohexomutase Superfamily. *Adv. Protein Chem. Struct. Biol.* **2017**, *109*, 265-304.